SEVENTH FRAMEWORK PROGRAMME

Report on Y2 activities and new integration strategy

FP7-ICT-216863/TUE/R/PU/D16.2

Project Number:	FP7-ICT-2007-1 216863
Project Title:	Building the Future Optical Network in Europe (BONE)
Contractual Date of Deliverable:	31/12/09
Actual Date of Delivery:	15/01/10
Workpackage contributing to the Deliverable:	WP16 : WP-VCE H (In-Building Networks)
Nature of the Deliverable	R (Report)
Dissemination level of Deliverable	PU (Public)
Editor:	Ton Koonen (TUE)

Abstract:
The activities in WP16, the Virtual Centre of Excellence on In-Building Networks, undertaken in BONE's second year are described. Based on the themes in the list of common interests, as identified in year 1, joint research activities have been executed in year 2. The joint research has been enforced by means of mobility actions, and has resulted in joint publications and exchange of personnel. In the final year, it is planned to continue and intensify joint research by means of mobility actions, to generate more joint publications in leading conferences and journals, and to safeguard the fruitful joint research cooperation established in in-building optical network technologies by means of new jointly proposed research projects (a.o. in FP7 Call 5).

Keyword list:
In-Building Networks, Joint Research, Mobility actions

Disclaimer

The information, documentation and figures available in this deliverable, is written by the BONE ("Building the Future Optical Network in Europe"*) – project consortium under EC co-financing contract FP7-ICT-216863 and does not necessarily reflect the views of the European Commission*

Table of Contents

1. Executive Summary

In BONE's second year (2009), according to the themes of common interest as identified and reported in D16.1 (see also Annex 1 to this deliverable D16.2).

In 2009, joint R&D activities in WP16 have taken place (and are being continued in 2010) regarding the various topical areas in WP16: optical network architectures and their techno-economics, radio-over-fibre in in-building networks (incl. digital radio schemes), wireless optics, high-speed data communication over SMF, MMF and POF using spectrum-efficient signal modulation schemes. In some more detail, the activities of WP16 partners in 2009 were:

- In-building network architectures: TUE and FT have made cost analyses of basic architectures for typical building scenarios, using SMF, MMF, POF and CAT-5E cabling. GET studied combinations of a POF backbone and free-space optic links.
- High capacity data transmission over wired links: TUE and UoA investigated advanced modulation techniques (OFDM, DMT, PAM, QAM) for Gbit/s transport over MMF and POF links. UoA studied modal dispersion mitigation techniques for SI-POF links. UCAM and UoA studied the impact of optical connectors. UCAM studied 40 and 100 Gbit/s Ethernet modulation schemes for SMF and MMF.
- Radio over fibre: UDE worked on 60GHz high-capacity systems. TUE, UDE, UCAM and UC3M worked on RoMMF and RoPOF systems. UVIGO studied WLAN use over RoF. TUE worked on OFDM-UWB and IR-UWB systems. UCAM studied RoF for localization and reading of passive RFID devices. UCAM studied the energy efficiency of wideband RoF systems, and low bit rate digital RoF systems.
- Flexible capacity allocation: TUE worked on wavelength routing of RoF signals.
- Sensor applications: UDE and UC3M worked on liquid level sensors. UC3M and Ericsson worked on new sensors for in-home networks.
- Wireless optical communication: FHG worked on visible light communication using white LEDs.
- Optical devices: UC3M and GET worked on liquid crystal switches. UDE worked on reflective electro-optic transceivers for RoMMF and RoPOF.

Several mobility actions have taken place to increase the interaction between the partners:

- Switching devices for in-home networks, PhD student from UC3M at GET,
- Incoherent spectral OCDMA experiments, PostDoc researcher from UAM at TUE,
- POF devices, PhD student from Ericsson at UDE,
- Teaching on optical sensors and home networks, associate professor from UC3M at GET.

A joint WP13/WP16 meting attended by all partners has been held in Poznan, Oct. 5, where the status of the WP16 activities has been discussed and new actions for the coming year have been agreed on.

Joint publications at many international conferences and in well-respected journals have been made. Also book chapters on optical components (including sensors) and on internet applications have been written.

Several partners are also involved in other FP7 projects which address in-building networks, notably ALPHA, MOEGA, FUTON, and POF-PLUS. There is a close cooperation and an active exchange of information with these projects. Amongst others, there was a joint booth in the exhibition area of ECOC 2009, displaying results of the in-building studies.

Moreover, WP16 partners have prepared jointly project proposals, amongst others in response to FP7 Call 5. As a result, it is expected that the cooperation between WP16 partners will continue after the final year of BONE, and thus also in the future contribute to strengthening the position of Europe's industrial and academic activities.

2. Introduction

The major objective of VCE-H is

To align the research activities on architectures and techniques for optical in-building networks,

by

- Co-ordinating and integrating research efforts, encompassing
- Exchange of researchers
- Joint research and laboratory experiments
- Joint publications
- Joint dissemination by means of workshops
- Establishing benchmark platforms for different optical in-building techniques
- Providing guidelines for roll-out and deployment of optical in-building networks, including migration paths

In this report, after describing the integration mechanisms in chapter 3, the joint research activities undertaken and the publications which resulted thereof are described in chapter 4. Furthermore, in chapter 5 the mobility actions are listed.

3. Mechanisms for Integration

The integration within this VCE-H is to be established by various ways of cooperation, based on an inventory of common interests among partners.

These co-operations encompass

- exchanging researchers by means of BONE's mobility programme, such that the experience of (young) researchers can be widened and the base of co-operation between research groups can be broadened
- joint research and laboratory experiments
- joint publications, at conferences and in journals or books
- jointly organizing dissemination events such as workshops etc.

It should be noted that several co-operations between partners have already been started within the preceding NoE e-Photon/ONe, within its Virtual Department VD-H on Home Networks. Within VCE-H, there is a further intensification of these co-operations, which also extends to other FP7 projects such as ALPHA, OMEGA, FUTON, POF-PLUS, etc., and to national projects.

In order to facilitate the integration among the VCE-H partners, the key research areas of common interest to the partners have been identified (as reported before in Milestone M16.1):

1. In-building optical network architectures, for integration of services, wired and wireless
2. Hybrid (optical/copper/wireless) in-building networks, upgrading
3. Management and control of in-building networks, ambient intelligence, control of resources, user-tailored services
4. Fault & performance monitoring + protection mechanisms, assure QoS, ease maintenance
5. Gateways access/in-building; interfacing, security, service adaptation, …
6. Interfacing with user terminals, matching I/O formats
7. Flexible capacity allocation, capacity and QoS on demand
8. Radio-over-single/multimode fibre, antenna remoting, CS consolidation
9. High capacity data over SMF/MMF, BW efficient modulation formats
10. Wireless optical communication, for pico-cells

11. Sensor applications (bursty, low data rate, multiple access)
12. Techno-economic analysis, to optimise system design
13. Safety and health aspects (a.o. eye safety, automatic shut-down)

The partners have been invited to indicate in which areas they are interested, and to describe these interests in more detail. The common interests of the partners are listed in the table shown in the Annex. Starting from this table, joint research activities have been initiated and executed, as well as mobility actions to exchange researchers.

3.1 Advisory Board

The following members were willing to provide their advice regarding VCE-H organizational and research directions, and to act as a liaison person to other BONE VCE-s and TP-s:

- John Mitchell (UCL; leader VCE-Access)
- Piero Castoldi (SSSUP; leader VCE-Services and Applications)
- Ioannis Tomkos (AIT; leader TP optical Communication Networks in support of user mobility and networks in motion)
- Achille Pattavina (PoliMI; leader TO Optical Interconnects)
- Maurice Gagnaire (GET)
- Stuart Walker (UEssex)
- Mario Pickavet (IBBT)
- Evi Zouganelli (Telenor)
- Juan Pedro Fernandez-Palacios Gimenez (TID)
- Mikhail Popov (ACREO; leader ALPHA)
- Andreas Stöhr (UDE; leader IPHOBAC)

4. Joint research activities

4.1 In-building optical network architectures

4.1.1 In-building optical network architectures for converged services delivery [TUE, FT]

Many different networks are currently being used for transferring all kinds of information in residential homes and in (semi-)professional buildings such as office buildings, hospitals, conference centres, airport departure halls, etc. Twisted copper pair cables are deployed for fixed-line and cordless telephones, and facsimile equipment. Coaxial copper cables deliver CATV and radio broadcast signals by connecting to (HD)TV terminals, radio tuners and video recording equipment. Cat-5 copper wire cables connect desktop PC-s, routers, hubs, printers and storage servers. Wireless LAN base stations support laptop computers, PDA-s, interactive gaming consoles, etc. Infrared and radio-based controllers are deployed for remotely steering TV sets, audio equipment, in-house lighting, etc. Other separate networks may be present for domotica applications (control of domestic appliances, heating, fire and burglar alarms, camera surveillance, etc.). As illustrated in Fig. 1.a, all these networks may co-exist next to each other, and are individually optimised for the functionalities they have to provide. On the other hand, this variety in networks implies quite a lot of effort for installation and maintenance. Also it may be difficult to introduce new functionalities such as those which become possible by making links between different service types; for instance, pausing a TV programme and/or lowering the audio volume of the TV set when you need to answer a telephone call.

A single network which can deliver all the above-mentioned services in an integrated way would considerably ease these issues. Optical fibre with its low losses and huge bandwidth is a promising transport medium for such a network, and can extend the capacity offered by the access network beyond the doorstep, into the building [1] , [2] . Its transparency for any signal-format, its small diameter and its immunity for EMC makes it a medium which can be installed virtually everywhere, and for any application. Fig. 1.b illustrates how an optical fibre network could connect all the rooms in a house to a centralized communication site, the residential gateway (RG). This RG can host all the communication functionalities needed to bring the various types of services to the various terminals in the house. It can also perform the signal format translation functions needed when for instance you want to watch a TV programme on your PDA, or want to watch on your HDTV screen a video game which you are playing on your laptop. It can also act as a local server where you can store (multimedia) information, such as data files, movies and music. Moreover, the RG is the bridge between the public access network and the private in-home network; it needs to do the necessary signal conversions, but also should guard your privacy and allow only authorized people to manage and update functions in your in-home network. The single fibre-based network can transport both the services for the wired terminals (large HDTV displays, desktop PC-s, telephone sets, …) and for the wireless ones (laptops, PDA-s, mobile phones, …).

In the following, we will discuss the various architecture options for the integrated in-building network and a first analysis of their economical aspects. The application area may be a small-scale residential home, or a larger (professional) building such as an apartment building, office building, hospital, etc. We also will address the suitability of the various fibre types available, and briefly review some recent research activities to carry high-capacity data streams for wired and wireless terminals over such networks.

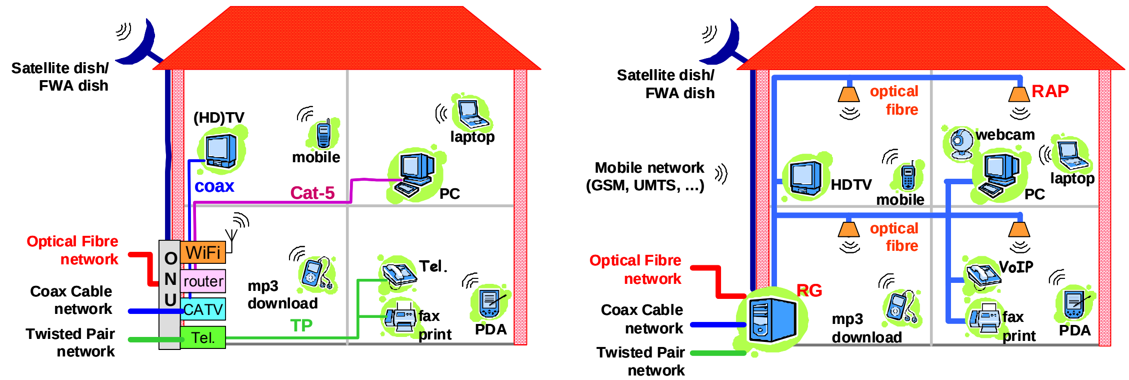

a) Today's separated networks

b) A single integrated network

Fig. 1 In-home communication networks

Basic architectures

Below, we will analyse a number of basic architectures according to which the integrated network may be laid out.

The most straightforward architecture is the point-to-point (P2P) architecture such as depicted in Fig. 2.a. Here an individual fibre connects the Home Communication Controller (HCC[1]) to each wall outlet in a room.

Alternatives to the P2P architecture can be offered by a number of point-to-multipoint (P2MP) architectures. In the tree architecture (Fig. 2.b), riser fibre cables may connect each floor of the building individually to the HCC, but per floor by means of a network splitter the wall outlets in the rooms are all fed from the same riser fibre. In the bus architecture (Fig. 2.c), each riser fibre cable is extended along the rooms on the respective floor, and each wall outlet is fed from an add-drop node inserted in this fibre line. Also combinations of the tree and bus architecture are obviously possible.

Fig. 2.d shows a multipoint-to-multipoint (MP2MP) architecture, where in a star-shaped network each wall outlet is connected by a single fibre to a star coupler device which is situated next to the HCC, or possibly at a more centralized site in the home. Such a star architecture allows direct communication between rooms without the intervention of the HCC.

The architectures may be implemented in two flavours: all-optical, or opaque. All-optical architectures transport the signals between the HCC and the wall outlets without any intermediate opto-electric-optical (O/E/O) conversion. The P2P obviously is an all-optical one. If optical power splitters and/or wavelength routers are used in the network nodes, P2MP and MP2MP architectures can also operate in the all-optical mode. Opaque architectures perform O/E/O conversion in the nodes, where the signal splitting/combining functions are done at the electrical signal level.

[1] The HCC basically hosts the same functionalities as the RG, but may also include some extra network control functionalities, such as the routing in point-to-multipoint architectures.

a) point-to-point

b) tree

c) bus

d) star

Fig. 2 In-building network architectures

When comparing these four basic architectures, a number of observations can be made, as listed in the following.

Amount of fibre and duct space needed

The P2P architecture requires a lot of fibre cables and duct space to host all this fibre. But network splitting nodes and comprehensive protocols to fairly share the access capacity to the fibre network among the wall outlets are avoided. The P2MP architectures save fibre and duct space, where the bus architecture uses the least. The MP2MP star architecture (with the star coupler located next to the HCC) uses about the same amount of fibre and duct space as the P2P one.

Number of network splitting devices

The P2P architecture obviously does not need network splitting devices, and the star architecture needs only one (with reflective-star functionalities when it should allow direct communication between rooms). The tree architecture uses one 1xN splitting device per floor, and the bus architecture uses the most (but simple) 1x2 splitting devices.

Fibre types

Three basic fibre types may be considered for in-building networks: silica single-mode fibre (SMF), silica multimode fibre (MMF), and polymer (large-core) multimode fibre (polymer optical fibre, POF). SMF has very low losses and an extremely large bandwidth; however, it is more difficult to install due to the accuracy needed when making fused fibre splices or connectorised fibre splices. New bend-insensitive single-mode fibre types have been developed which allow small bending radii and thus support installation in curved ducts. MMF has a smaller bandwidth than SMF due to its modal dispersion, but is easier to splice thanks to its larger core diameter. Graded-index MMF has been widely installed in office buildings, and its bandwidth is significantly larger than that of step-index

MMF. Large-core POF (in particular 1mm core diameter PMMA step-index POF) is very easy to splice and to couple to optical sources, as well as to pull through ducts because of its ductility. It is suited for do-it-yourself installation, as it does not require precision techniques nor skilled personnel for splicing.

Network splitting functions, such as power splitting and wavelength routing, are readily available in single-mode fibre based devices. With multimode fibre, such functions are harder to realise; any mode-selective process should be avoided as it will introduce modal noise (which is signal-dependent and thus leads to bit error rate floors). When using bulk optics lenses and beam splitters, non-mode-selective optical splitters can be built; up to now, these have been mostly realized for laboratory application only.

Scaling the network to more wall outlets

In order to increase the number of wall outlets, in the P2P architecture and in the MP2MP star architecture new fibres (and possibly new ducts when the available duct room is no longer sufficient) need to be installed, both in the vertical riser part of the network and the horizontal part. In the tree architecture, new fibres (and possibly ducts) need to be installed per floor, so only in the horizontal part; moreover, the number of ports of the network splitter needs to be enlarged. In the bus architecture, only simple 1x2 network splitters need to be added (and maybe a bit of horizontal fibre cabling). Both in the tree and the bus network, after upscaling the riser fibre will be shared by more wall outlets, so when the resources in the network (i.e. the number of time slots, or of frequency band slots) stays unaltered the capacity available per wall outlet will decrease.

Upgrading with additional/enriched services

All-optical network architectures are fully transparent for the signal formats they have to carry; introducing new services or extending the existing ones is relatively easy, as it mainly requires upgrades of the line termination equipment only. Hence the P2P architecture enables easy upgrading, and the all-optical bus, tree and star architectures also. By using a reflective all-optical star coupler, the star network supports transparent all-optical communication directly between the wall outlets, without intervention of the HCC. Bi-directional communication may be implemented by using a single fibre per wall outlet and separating up- and down-stream traffic by (coarse) wavelength multiplexing, or by duplex fibre cables (and thus twice as much fibre in the network, plus more duct space).

When the bus, tree and star architectures are opaque, the upgrading may require considerably more effort, as all the intermediate O/E/O nodes may require upgrades of their internal electronic functions. For instance, when the nodes in the opaque architecture are IP-based it is not easy to introduce non-IP based services.

Support for wired as well as wireless services

The delivery of wired as well as wireless services must be facilitated by the HCC. In the so-called femto-nodes approach, the 3G wireless base stations throughout the building are fed by IP-based signals, and the radio carrier generation and modulation is done in the base station. Thus for both the wired and the 3G wireless services delivery, an all-IP network suffices, such as opaque network architectures with IP-based nodes. When higher wireless capacities are needed, wireless pico-cells may be introduced which use microwave frequencies (such as 60GHz) or ultra-wideband (UWB) short reach radio techniques. To avoid the comprehensive and costly microwave carrier generation and modulation per pico-cell antenna, the generation and modulation may be consolidated in a centralized site (e.g. next to the HCC), from where the modulated radio signals are brought by the fibre network to the simplified antenna stations. This radio-over-fibre (RoF) approach implies the transport of (microwave) analog optical signals over the fibre network. Advanced RoF techniques such as the Optical Frequency Multiplying technique enable the delivery of high-capacity wireless services even over dispersive multimode fibre networks [3] . Advanced multitone multilevel modulation techniques also allow very high data rates for wired services over multimode fibre [4] . In order to combine transport of wireless services together with transport of the (IP-based) wired services, the network preferably should be an all-optical one; it is considerably more complex to realise this approach in an opaque architecture.

Dynamically reconfigurable in-building network architectures

In particular in (semi-)public larger buildings, the traffic demands throughout the building may show spatial fluctuations. E.g., in a university building the traffic demand may be high in lecture rooms when many students are attending a lecture, whereas the demand may shift to other rooms in the building when students are migrating to other rooms for e.g. laboratory exercises. Similar traffic shifts may occur in the various departure rooms of an airport where people are waiting and are making phone calls and/or are using internet access with their laptops. To make the most efficient use of the installed resources in the overall network, it would be advantageous when the available capacity of the network can be directed to those places where there is an actual demand, thus redirecting unused capacity to where it can be used, instead of offering the capacity everywhere without taking the demand into account. By means of optical routing such a capacity-on-demand approach may be realized in an all-optical network architecture. By using multiple wavelength channels in the architecture, different types of services can be hosted in the network, including wired services using particular multilevel modulation formats to attain a high capacity, next to radio-over-fibre signals for high-capacity pico-cell wireless services. Wavelength routing of these channels opens the road to capacity-on-demand allocation.

For the all-optical P2MP architectures (bus and tree), optical routing can be accommodated in the splitting nodes. They can add flexibility in the network and thus provide capacity and QoS to the wall outlets where needed; this improves the efficiency of the available network resources. As depicted in Fig. 3, by using multiple wavelengths we can create separate wavelength planes which each constitute an interconnection pattern between the HCC and the various wall outlets. By deploying adaptive wavelength routing functions in the network splitting nodes, the interconnection patterns can be changed on demand. These routing functions can be implemented with wavelength add-drop-continue modules, and with wavelength crossconnect modules. Such modules (with larger numbers of input and output ports) are presently being deployed in metro-access and metro-core networks, but significantly cheaper solutions may be created for in-building deployment.

For the MP2MP architecture (star), flexible wavelength routing deploying a wavelength crossconnect can yield reconfigurable inter-room communication patterns; see e.g. the architecture in Fig. 4.a [3] . Alternatively, deploying an optically transparent star-shaped power splitter near the gateway, a wavelength-broadcast-and-select architecture can be realized (see Fig. 4.b, and [5]): every wall outlet receives all wavelengths, and (remotely controlled) wavelength selection functions at those outlets determine the wavelength interconnection patterns (cf. Fig. 3).

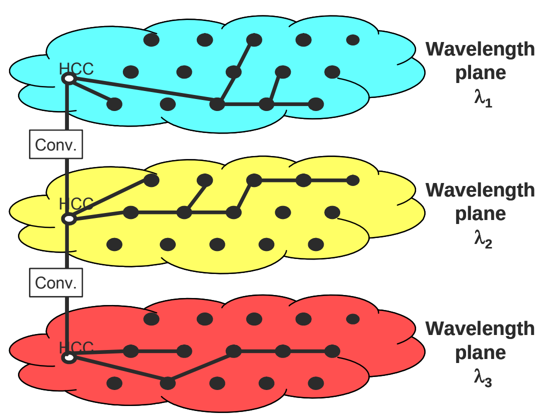

Fig. 3 Wavelength-defined subnetworks

Optical broadcast-and-select is power-hungry, and hence more suited for smaller buildings. Optical routing implies a more efficient use of optical power, and thus a better link power budget; hence it is more suited for larger buildings. The optical add-drop-continue functions and optical crossconnect functions are available in single-mode fibre-based modules (although not at the appropriate price level yet). They are not (yet) readily available in multimode silica nor polymer fibre-based modules. Hence the optical dynamic routing concepts are mainly intended for larger in-building networks, based in silica single-mode fibre.

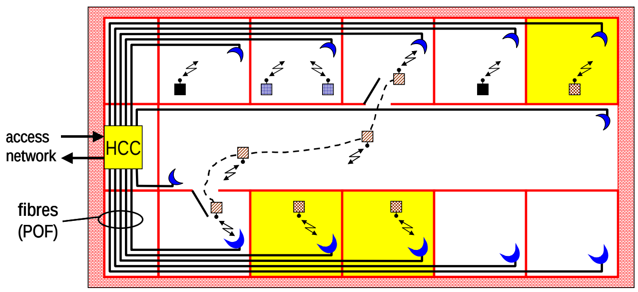

a) wavelength routing

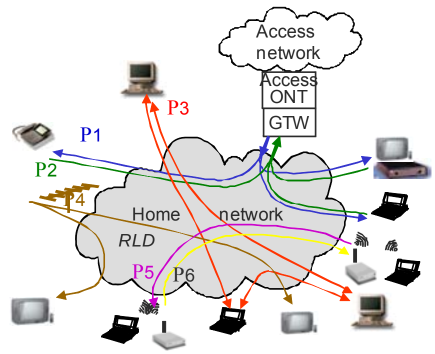

b) wavelength broadcast & select

Fig. 4 Reconfigurable inter-room communication

Conclusions

By deploying optical fibre, an in-building network can effectively integrate the delivery of high-capacity wired and wireless services in a single infrastructure. The choice for the network architecture may not be a "one-size-fits-all". In a relatively small residential home, a point-to-point architecture using do-it-yourself large-core POF may be attractive, whereas for a more demanding and more professional large building a point-to-multipoint architecture (and in particular a bus architecture) using the ultimate-capacity bend-insensitive single-mode fibre may be preferred. When implemented all-optically, dynamically controlled optical wavelength routing may enable delivery of capacity-on-demand and thus optimize the utilization efficiency of the network's installed resources.

References

[1] P. Chanclou et al, "Optical access evolutions and their impact on the metropolitan and home networks", Proc. ECOC 2008, Brussels, Sep. 21-25, 2008, paper We.3.F.1

[2] A.M.J. Koonen, "Trends in optical access and in-building networks", Proc. ECOC 2008, Brussels, Sep. 21-25, 2008, tutorial paper We.2.A.1

[3] A.M.J. Koonen, M. García Larrodé, "Radio-over-MMF techniques – Part II: microwave to millimeter-wave systems", IEEE J. of Lightwave Technol., 2008, Vol. 26, No. 15, pp. 2396-2408

[4] H. Yang, S. C. J. Lee, E. Tangdiongga, F. Breyer, S. Randel, A.M.J. Koonen, "40 Gb/s Transmission over 100m Graded-Index Plastic Optical Fiber Based on Discrete Multitone Modulation, Proc. OFC 2009, San Diego, Mar. 22-26, 2009, post-deadline paper PDPD8

[5] H. Ramanitra, P. Guignard, A. Pizzinat, "Scalable Optical Multi-service Home Network", Proc. OFC 2008, San Diego, Feb. 24-28, 2008, paper JThA90

4.2 *Hybrid (optical/copper/wireless) in-building networks*

No activities of partners reported.

4.3 Management and control of in-building networks

No activities of partners reported.

4.4 Fault & performance monitoring + protection mechanisms

No activities of partners reported.

4.5 Gateways access/in-building

No activities of partners reported.

4.6 Interfacing with user terminals

No activities of partners reported.

4.7 Flexible capacity allocation

4.7.1 All-Optical Multicasting of Millimetre-Wave Signals using Optical Frequency Multiplication Technique for In-building Networks [TUE]

The combination of mm-wave technology with Radio-over-Fibre (mm-RoF) has emerged as a key technology for in-building networks [1] [2] . By means of mm-RoF, picocells in a building can be extended to several rooms instead of having a single large wireless network, which covers the whole building and might cause interference problems. Recent proposals for in-building networks have suggested that radio signals (or baseband signals) are broadcasted through an optical fibre and the channel selection is made at each destination (room). However, with broadcast-and-select configuration, there are concerns regarding high power consumption and security.

Below, we demonstrate a new optical frequency multiplication (OFM) configuration [3] for in-building networks illustrated in Fig. 5. The key functionalities of the proposed architecture are simultaneous all-optical mm-wave generation, multicasting and selective routing of the mm-wave signals to individual rooms based on encoded header information [4] . This centralized optical routing can dynamically adjust the optical connectivity and RF frequency allocation. Hence the radio-cells can be dynamically adjusted in size and capacity, which improves the traffic handling capacities and network operational efficiency. In addition, the selective optical connectivity prevents unnecessary power consumption and offers enhanced security. As a proof of concept, we successfully demonstrated photonic up-conversion of 3.6GHz radio signal carrying 20MSymbols/s 64-QAM data to 39.6GHz mm-wave frequency, and selective optical multicasting of four wavelength channels with mm-wave signals. Each wavelength channel showed an error vector magnitude (EVM) of 4.5% at 39.6GHz.

Multicasting of mm-wave signals using OFM technique

Fig. 5 illustrates the in-building network scenario. An optical transparent gateway routes or multicasts wired radio signals (or baseband signals) from the central station (CS) to each room carried on a mm-wave carrier signal. The system consists of a WDM source, a phase modulator, a 3-dB coupler, a semi-conductor optical amplifier (SOA), a Mach-Zehnder Interferometer (MZI), and an optical router based on an arrayed waveguide grating (AWG). Several continuous wave (CW) optical signals ($\lambda_{1\text{-}4}$) from WDM source, which are selected based on the address information extracted from the downstream optical signal [4], are phase-modulated (PM) by the RF sweep signal (f_{SW}) to generate optical harmonics [3]. These PM optical signals ($\lambda_{1\text{-}4}$) are injected into the SOA together with the intensity-modulated (IM) optical signal (λ_{MOD}) carrying the radio signal from the CS. By cross-gain modulation (XGM) in the SOA, the radio signal is duplicated onto the PM optical signals ($\lambda_{1\text{-}4}$). In the MZI, PM-IM conversion allows the mm-wave carriers at the multiples of the RF sweep frequency (f_{SW}) to appear at each optical wavelength ($\lambda_{1\text{-}4}$) as illustrated in Fig. 5.

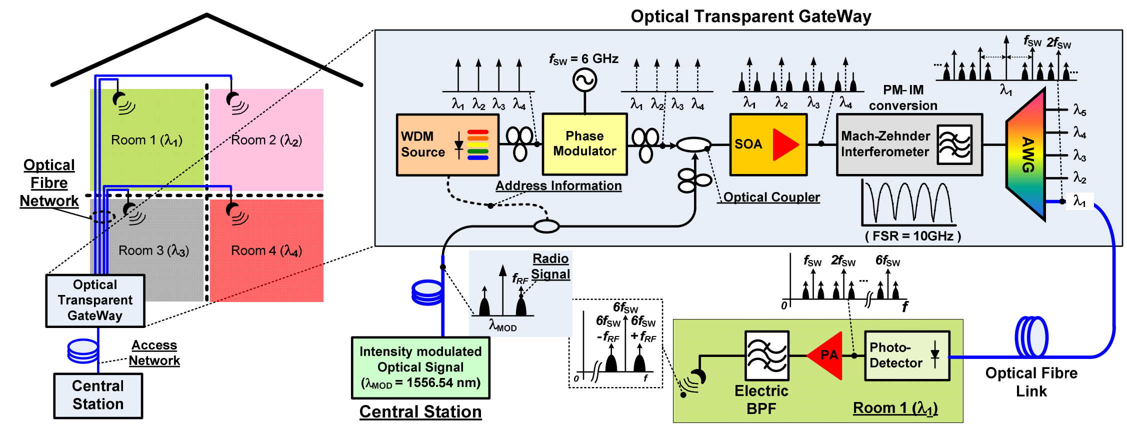

Fig. 5 Concept and Experimental Setup (Radio Signal from the central station: 64-QAM, 20Msymbols/s at 3.6GHz RF carrier)

The converted optical signals ($\lambda_{1\text{-}4}$) are routed by means of an AWG to each destination, where they are detected and the mm-wave radio signal is selected by a bandpass filter (BPF).

Results and discussion

To generate mm-wave carrier signal, CW optical signals ($\lambda_{1\text{-}4}$) from a WDM source were phase-modulated with a 6GHz RF sweep signal (f_{SW}). The CW wavelengths ($\lambda_{1\text{-}4}$) were selected by header processing based on the address information extracted from the IM optical signal (λ_{MOD}) [4]. Fig. 6(a) shows the RF spectra of the multiple harmonics generated by the OFM technique [3]. The PM optical signals were inserted into the SOA with the IM optical signal carrying the radio data signal (f_{RF} = 3.6GHz) shown in Fig. 6(b). Then, the radio signal was duplicated (wavelength-converted) on each PM optical channel and optically up-converted along with the harmonics of f_{SW} to $f_{UP}=n{\bullet}f_{SW}\pm f_{RF}$ (where n is the order of harmonics) by XGM of the SOA; Fig. 6(c) depicts the radio signal up-converted to f_{UP}=39.6GHz ($n=6$). As shown in Fig. 6(c), the SNR of the received mm-wave signal is reduced by around 16dB and the EVM penalty is 2.5%, compared to the input RF signal. In addition, a non-linear skirt slope appears at the edge of the signal band. This degradation comes from the ASE noise of the SOA, the wavelength-conversion penalty, and the nonlinearity of the SOA gain profile.

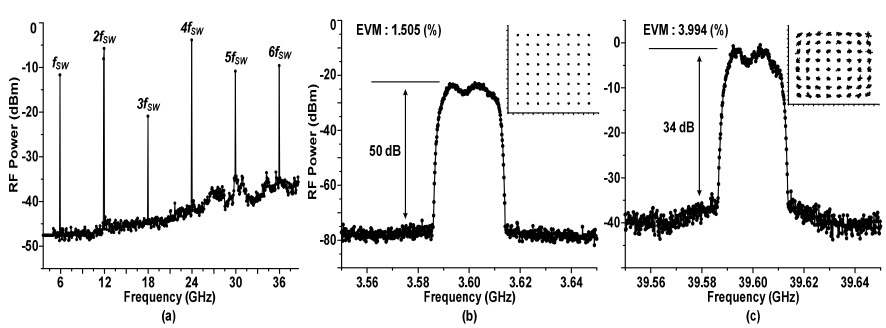

Fig. 6 RF spectra of (a) multiple harmonics generated with RF sweep frequency (fSW=6GHz), (b) input 64-QAM signal (20MS/s) at 3.6GHz, (c) received 64-QAM signal (20MS/s) at 39.6GHz (Inset: constellation diagram)

Fig. 7 shows the performance of the optical multicast for mm-wave signal at each channel. Firstly, we observed the influence of the number of optical channels to the SOA. Notice that in Fig. 7(a), the EVM performance at λ_1=1550.735nm is slightly degraded when increasing the number of input PM optical channels. This is due to the gain competition between the channels in the SOA; the reduction of optical gain by the adjacent channel decreases the efficiency of XGM. Thus, for multicast, Fig. 7(b) indicates that the channel spacing is set to maximize the number of available channels while minimizing inter-channel interference.

The EVM performance of the routed mm-wave signals at each wavelength-channel is nearly the same, with around 4.5% as shown in Fig. 7(c). Fig. 8 shows the optical spectra of all optical channels including the IM signal from the CS. Also the products from four-wave mixing (FWM) can affect the EVM performance. These unwanted products are filtered out by MZI or AWG. Therefore, assuming a limited number of optical channels such as in a small-scale in-building environment, the proposed all-optical multicasting system for mm-wave signals is a simple and robust solution.

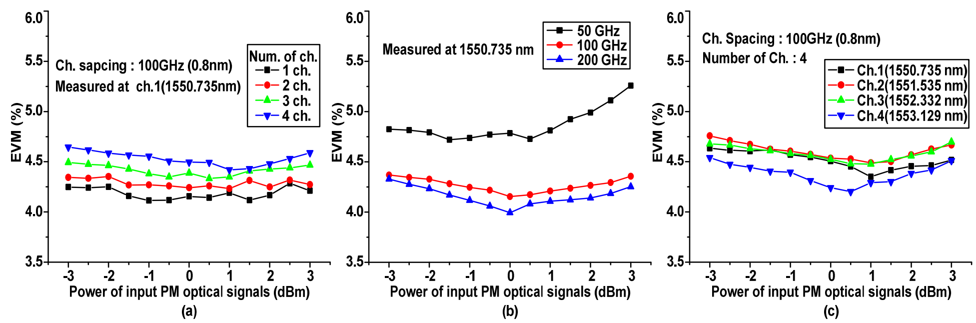

Fig. 7 Performance of multicast: the influence of (a) number of input optical Ch. to SOA, (b) channel spacing, (c) performance of routed mm-wave signal at each Ch. (the power of input IM optical signal fixed at +3dBm)

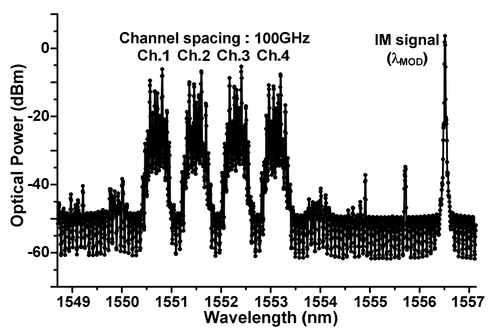

Fig. 8 Optical spectrum of multicast optical channels

Conclusions

In this paper, we proposed a new configuration for all-optical multicast of mm-wave signals using the OFM technique for in-building environments. By using XGM in an SOA, we can optically up-convert radio signals at low frequency to the mm-wave frequency region and convert radio signals to different wavelength channels at the same time. In the experiment, we successfully demonstrated photonic up-conversion from a 3.6GHz radio signal carrying 20MS/s 64-QAM data to a 39.6GHz mm-wave frequency and optical multicast of four wavelength channels with the mm-wave signal to different destinations. At the receiver side, each wavelength channel showed nearly the same EVM performance of 4.5% for 20MS/s 64-QAM data at 39.6GHz.

References

[1] A.J. Seeds, IEEE Trans. Microw. Theory Tech., 50, 877 (2002).

[2] L. Noel et al., IEEE Trans. Microw. Theory Tech., 45, 1416 (1997).

[3] A.M.J. Koonen and M. Garcia Larrode, J. Lightw. Technol., 26, 2396 (2008).

[4] H.-D.Jung et al., Proc. ECOC 2008, Tu.4.F.2 (2008).

4.8 Radio-over-single/multimode fibre

4.8.1 Super-broadband photonic wireless system demonstrations [UDE, FT]

University Duisburg-Essen and France Telecom have realized a super-broadband 60 GHz photonic wireless system and demonstrated wireless transmission with a world record data throughput and spectral efficiency of 27 Gb/s and 3.86 bit/s/Hz [1]. The compact system is based upon a cascaded RF and data modulation approach. By using an 8-QAM and 16-QAM OFDM modulation format we achieved record spectral efficiencies up to 3.86 bit/s/Hz. Experiments have been carried out with 10 m fiber-optic and 2.5 m wireless transmission. For 8-QAM OFDM modulation a data rate of 20.28 Gbit/s with a measured mean EVM of 18.8 % and a SNR of 18.9 dB resulting in a BER of 2.2·10-4 has been achieved. For 16-QAM OFDM modulation a record throughput of 27.04 Gbit/s was successfully achieved. In that case, the measured mean EVM and SNR were 17.6 % and 21.5 dB, respectively resulting in a BER of 4.2·10-3 which is slightly above the FEC limit. The transmit power and antenna gain used in the experiments were -1 dBm and 23 dBi, respectively. By increasing the transmit power and antenna gain, we expect being able to extend the wireless span up to a few 100 m given the measured wireless receiver sensitivity

References

[1] M. Weiß A. Stöhr, F. Lecoche, B. Charbonnier, 27 Gbit/s Photonic Wireless 60 GHz Transmission System using 16-QAM OFDM, International Topical Meeting on Microwave Photonics, MWP 2009, Oct. 14-16, Valencia, Spain, 2009, (post deadline paper)

4.8.2 In-building RoMMF links with reflective electro-optic transceiver [UDE, UoEssex]

The use of a passive, low-power and low-cost optoelectronic WDM transceiver at the base-station, containing a modulator (modulation wavelength 790nm, quasi-transparent at 850nm) super-integrated with a PD (850nm) for single-fibre uplink RoMMF transmission has been successfully demonstrated. With this Reflective Electro-Optic Transceiver (REOT) error-vector-magnitude (EVM) measurements for multi-standard and subcarrier-multiplexed (SCM) wireless signals have been carried out with a link shown in Fig. 9[2].

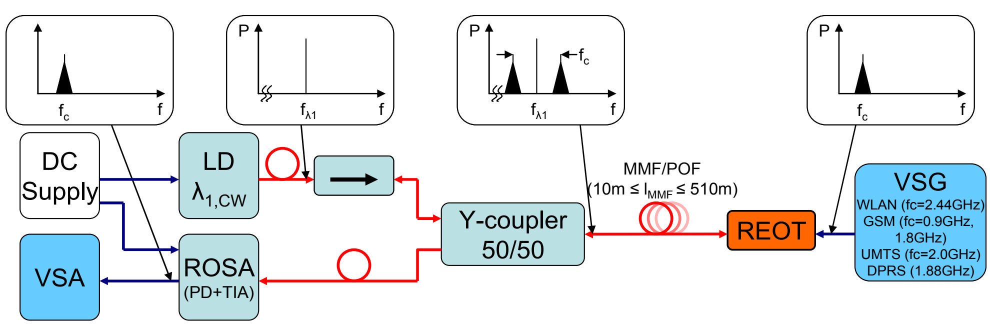

Fig. 9 System block diagram for RoMMF uplink measurements using the modulator function of the REOT

A RoMMF link with the REOT device (here the reflective electro-absorption modulator based on a asymmetric Fabry-Perot modulator with bragg mirrors) was set up for EVM uplink measurements of multi-standard wireless access signals. All fibers used were 62.5µm core diameter with graded-index (GI) profile. A continuous wave signal, provided by a fiber pigtailed edge emitting LD ($\lambda 1$ = 790 nm, Popt = 5.8 dBm @ 110 mA), is guided through an optical isolator and y-coupler, multimode glass optical fiber (MM-GOF), over different lengths and types of MMF/POF fibers. A MM-GOF pigtail bare end is free-space coupled to the REOT device. An Agilent vector signal generator (VSG) E4438C is directly connected to the REOT modulator with 0 V bias using microprobe contact equipment. The modulated signal is received by the same fiber and guided through the y-coupler to a ROSA package (f3dB,ROSA = 9 GHz). The demodulation was provided by an Agilent MXA N9020A vector signal analyzer (VSA).

RoMMF data transmission measurements were carried out for different wireless standards, lengths and types of fibers. Table 1 summarizes the EVM measurement results for different wireless standards such as GSM (GSM900 and DCS1800), DPRS (DECT), UMTS, and WLAN 802.11 b/g. It can be seen that the EVM requirements for all GSM, UMTS, DPRS and WLAN 802.11b transmissions can, to some extend, be highly exceeded with the proposed system. Selected constellation diagrams are displayed in the last column of Table 1.

Table 1 EVM requirements and measured results of IEEE and ETSI standard signal transmission using the proposed uplink with a GOF length of 25 m

Standard (Technique)	Modulation Format	Carrier Frequency	Chip / Data Rate	Filter	Required EVM (%rms)	Measured EVM (%rms)	Constellation Eye Diagrams
GSM 900 (TDMA)	GMSK	900 MHz	270.833 kbps	BT= 0.3	< 7.0	1.19	
DCS1800 (TDMA)	GMSK	1800 MHz	270.833 kbps	BT= 0.3	< 7.0	1.74	
DPRS (TDMA)	64QAM	1.88 GHz	1.152 Msps	α = 0.5	< 2.6	2.51	
UMTS (WCDMA)	QPSK	2 GHz	3.84 Mcps	α = 0.22	< 12.5	2.61	
WLAN 802.11b (DSSS)	QPSK	2.45 GHz	11 Mbps	α = 0.3	< 35	6.82	
WLAN 802.11g (OFDM)	64QAM	2.45 GHz	54 Mbps	α = 0.3	< 5.6	9.79	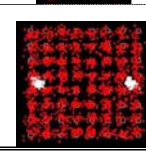

In order to relate the link performance to carrier frequency up to 5 GHz EVM/SNR vs. frequency measurements were carried out applying a 16QAM 24 Mbps (6 MHz modulation bandwidth) signal (Fig. 10.a). By adjusting the applied modulator input power for each measurement point separately EVM values below 5 %rms were recorded up to carrier frequencies of 3.5 GHz. This allows IEEE 802.16e WiMAX WCDMA transmission (Germany: 3.4 GHz - 3.6 GHz) with medium data rate performance. For in-building scenarios different types of fibers and lengths will be of interest for such RoMMF systems. Therefore we investigated the influence of fiber types of 62.5µm GI-GOF and 62.5µm perfluorinated (PF)-GI-POF and lengths for the system, respectively. A QPSK signal at a carrier frequency of 2.44 GHz with a data rate of 2 Mbps was used for EVM analysis. The results of the measurement are summarized in Fig. 10.b.

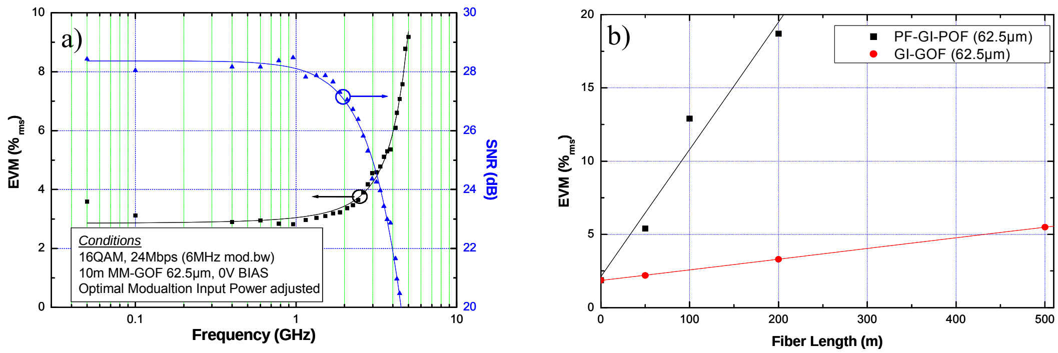

Fig. 10 (a) EVM/SNR vs. carrier frequency, 16 QAM, 24Mbps, 0V Bias at Modulator, Modulation Input Power adjusted (range: 3 dBm to 13 dBm), (b) EVM measurement results for different lengths (excluding pigtail fiber of 10m MM-GOF) of MM-GOF and MM-POF with a QPSK 2Mbps at 2.44GHz carrier frequency [3]

For both fibers we obtain a somehow linear correlation of fiber length and EVM value for this uplink system. The comparison of both slope values for the different fibers shows ten times higher slope in PF-GI-POF compared to GI-GOF. The difference of NA between both fibers (PF-GI-POF and pigtail GI-GOF) results in coupling losses at both, the y-coupler and to the pigtail fiber of the REOT causing signal loss and EVM rising. For all measurements a broadband circulator for a wavelength range from790 nm to 850 nm could increase link performance significantly due to optical loss reduction by y-coupler and isolator. Coupling efficiency of the REOT to the fiber and modulator matching or matched driving circuitry could further improve measurement results.

We have proposed a RoMMF transmission system using a passive bidirectional full-duplex transceiver for eo-conversion at the base station for the first time. EVM analysis show that multiple standard wireless access signals such as GSM, UMTS, WLAN 802.11b and WiMAX can be transmitted with values partially far below the required ones according to the standards. Different scenarios on fiber type and length were tested in order to demonstrate their dependence for in-building installations [3]. In addition, distributed-antenna-system (DAS) infrastructures with coax, SMF, MMF, and POF have been compared with respect to installation effort, CAPEX, and system dynamic range (SDR) [4].

References

[1] I. Möllers, D. Jäger, “Transparent Radio-over-Multimode Fiber Transmission System with Novel Transceiver for Picocellular Infrastructures“, 35th European Conference and Exhibition on Optical Communication (ECOC 2009), Vienna, Austria, September 20-24, 2009

[2] I. Möllers, D. Jäger, “Bidirectional Multi-Standard RoMMF Transmission Using a Reflective Electro-Optic Transceiver”, European workshop on photonic solutions for wireless, access, and in-house networks, Duisburg, Germany, 2009

[3] M.C. Parker, S.D. Walker, R. Llorente, M. Morant Pérez, M. Beltrán Ramírez, I. Möllers, D. Jäger, C. Vázquez, D.S. Montero, I. Librán, S. Mikroulis, S. Karabetsos, A. Bogris, “Radio-over-Fibre technologies arising from the Building the future Optical Network in Europe (BONE) project, submitted to IET Optoelectronics Journal – Special Issue on Next Generation Optical Access, July 2009

4.8.3 Switching devices for RoF in-home networks [UC3M, GET]

Design and integration of transparent NxN fiber switches for controlling the inter-room communications between Radio-over-Fiber links are under study.

Those multimode fiber switches will be based on LCs, so LC cell fabrication and characterization is developed; oriented to their application as part of those switching devices to be used in in-home networks for keeping connectivity between different rooms. Those rooms will have broadband access capability by using RoF to reach each pico-cell at each individual room.

This device will perform some of the functionalities reported in [1] if available.

A multifunctional device able to switch by splitting and attenuating has been developed and characterized. It is a combination of a multiplexer and a variable optical attenuator in the same device (VMUX) for being used in Polymer Optical Fiber. Polymer Dispersed Liquid Crystals (PDLC) technology is used as switching elements in the device; being polarization independent, having high contrast and gray scale capability. Characterization of the PDLC cells has been carried out at two wavelengths. VMUX Complete switching is reached for driving voltages of 20Vrms, with insertion losses less than 1.6dB, attenuation larger than 31dB, rise time less than 2.6ms and decay time better than 12.4ms have been obtained [2].

A review of different LC technologies as switching elements have also been carried out, including those hybrid applications with POF technology [3].

Another way of providing space-connectivity between MM fiber arrays is to use free-space connections (or switching). The main advantage with this technique is that the number of fibers that could be connected is probably much larger than with the solution currently developed. Some experiments to confirm this will be designed.

References

[1] Koonen, A.M.J., Garcia Larrode, M., Ng'Oma, A., Wang, K., Yang, H., Zheng, Y., Tangdiongga, E. (2008). Perspectives of radio over fiber technologies. Proceedings of the Optical Fiber Communication and National Fiber Optic Engineers Conference (OFC/NFOEC 2008). (pp. OThP3). San Diego

[2] P. C. Lallana, Carmen Vázquez, B. Vinouze, K. Hegartty, David Sánchez Montero, "Multiplexer and Variable Optical Attenuator based on PDLC for Polymer Optical Fiber networks" *Journal of Molecular Crystals and Liquid Crystals*, 502, 130-142, 2009

[3] *Optical switches: materials and design.* Book editors: Soo Jin Chua and Baojun Li, U. Singapore chapter 9 "Liquid Crystal Optical Switches" Carmen Vázquez, I. Pérez, P. Contreras, B. Vinouze, B. Fracasso. Editorial: © Woodhead Publishing Ltd, 2010

Outcomes of the joint research activity:

- 1 paper in a JCR journal (ref. :[2])
- 1 book chapter to be published (ref. [3])
- a chapter book will be published.

4.8.4 RoMMF Temperature influence (also in WP-13) [UC3M, UDE, UPVLC]

Multimode optical fibre has several advantages for short-reach applications compared to singlemode optical fibre because it is easier to fabricate, to connect and to manipulate (allow less stringent alignment tolerances thanks to its larger core diameter). Nevertheless, its main disadvantage is the reduced bandwidth limited by the intermodal dispersion. In order to get the maximum performance in MMF links the availability of accurate models to describe the signal propagation through multimode fibres are required. For the analysis of signal propagation through MMF fibres, a closed-form analytic expression to compute the baseband and the RF transfer function of a MMF link based on the electric field propagation method is presented in [1].

In addition to the bandwidth limitation by the intermodal dispersion in multimode fibres, the frequency response of multimode fibre links depends, in general, on the launching conditions due to excitation-dependent modal group delays and on mode group coupling [1, 2]. Therefore, launching conditions, variable link lengths, installation bends, connector offsets or the introduction of any other component along the multimode fibre link makes the multimode fibre frequency response unpredictable under arbitrary operating conditions, which imposes a great challenge for the extension of the bandwidth-dependent radio-over-multimode-fibre performance. Variations on temperature have also been demonstrated to change some of the optical properties of multimode fibres [3] and, consequently, it is clearly necessary to estimate their effect over the broadband transmission bands in a RoF system. Those systems can be integrated with fiber-optic sensors networks at remote operation [4] which can be expose to considerable temperature gradients.

Temperature dependence of the bandwidth in a RoF multimode silica fibre link has been experimentally tested when environmental temperature changes. The measurements are taken at temperatures from T=28ºC (environment) to T=67ºC. The hysteresis cycle of the measurements has also been evaluated at the environmental temperature.

A multimode silica optical fibre link has been implemented to experimentally validate the influence of temperature in the proposed model described in [1]. A Fabry-Perot optical source at 1300nm (Agilent 81655A) modulated up to 20GHz by a Lightwave Component Analyzer (LCA, Agilent 8703B) has been employed to launch optical power into the fibre. The optical power at the end of the fibre is, then, collected by a wide bandwidth InGaAs PIN photodiode and, finally, analyzed in terms of the frequency response by the LCA. MMF specifications were 62.5/125µm (core/cladding fibre diameters), n_{core}=1.4558 (refractive index in the core center), $n_{cladding}$=1.4472 (cladding refractive index), Δ=0.0059 (refractive index contrast between the core center and the cladding), and α_m=0.7dB/Km (fibre attenuation).

Several temperatures have been tested for a L=3050m MMF fibre link at λ=1300nm up to 20GHz with an average factor of Avg=16 at each temperature test measurement. Test equipment was isolated from the heating source thus affecting the temperature deviation only to the MMF fibre spool. Results can be seen in [5].

References

[1] I. Gasulla and J. Capmany: Transfer function of multimode fibre links using an electric field propagation model: Application to Radio over Fibre Systems, *Opt. Express*, vol. 14(20), pp. 9051-9070, Sept. 2006.

[2] L. Raddatz and I. H. White,"Overcoming the Modal Bandwidth Limitation of Multimode Fiber by Using Passband Modulation" IEEE Photonics Technology Letters, Vol. 11, No. 2, 266-268, Feb.1999.

[3] G. Rajan, Y. Semenova, P. Wang and G. Farrell: Temperature-Induced Inestabilities in Macro-Bend Fibre Based Wavelength Measurement Systems, J. Lightwave Technol., Vol. 27, No. 10, pp. 1355-1361, 2009.

[4] J. Montalvo, C. Vázquez, and D. S. Montero, "*CWDM self-referencing sensor network based on ring resonators in reflective configuration*," Opt. Express 14, n.11, 4601-4610, 2006

[5] D.S. Montero, I. Gasulla, I. Möllers, D. Jäger, J. Capmany and C. Vázquez "Experimental analysis of temperature dependence in multimode optical fiber links for Radio-over-Fiber applications"11th International Conference on Transparent Optical Networks ICTON 2009, 2009.

Outcome of the joint research activity:

- 1 joint paper in a conference (ref. [5])

- a new publication is under development

4.8.5 Generation and Transmission of FCC-Compliant Impulse Radio Ultra Wideband Signals over 100-m GI-POF [TUE]

The increasing demand for high-bandwidth multimedia wireless services is hampered by the lack of available spectrum. The short-reach Ultra Wideband (UWB) technology was adopted by the US Federal Communications Commissions (FCC) as an attempt to make more radio spectrum available. UWB technology combined with optical fibers for reach extension may provide an attractive solution for high-speed data access for mobile/nomadic users at home [1]. The selection of the impulse signal type is important as it determines the performance of UWB systems. As described in [2], Gaussian monocycle pulses and doublets can provide better bit-error rates and multipath resilience among different impulse signals. Basically, these waveforms can be created by a sort of band-pass filtering of a Gaussian pulse, i.e., filtering acts in a manner similar to differentiating the Gaussian waveforms. However, these widely used pulses do not fully satisfy the FCC rules. Hence, different pulse design techniques have been proposed recently such as the pulse design technique in [3],[4].

Below, we propose a new approach to generate an UWB pulse based on the concept of linear combination of 3rd order derivatives of a Gaussian pulse. Since differentiation is a way to move energy to higher frequency bands, we exploit pulse design techniques proposed in [3] to design pulses with better transmitted powers than the widely adopted Gaussian pulses, while respecting the FCC mask.

IR-UWB transport using plastic optical fibers

For large-scale short-range applications, multi-mode fibers (MMFs) offer the advantage of easy installation as their larger core diameter and numerical aperture allow large alignment tolerances. More importantly, plastic optical fibers (POFs) can enable short low-cost broadband transmission links, such as in in-home networks. When compared to silica MMFs, graded-index POF (GI-POF) offers further advantages such as smaller bending radius (<5mm), better tolerance to tensile load and stress, and simpler connectorization [5]. Therefore, impulse radio UWB (IR-UWB) over GI-POF provides an attractive solution for in-building networks.

Theory and experiments

We consider a weighted sum of two third-order derivatives of Gaussian pulses with different pulse-shaping values of σ_{31} and σ_{32}. The weighted sum value $y_{ws3}(t)$ is given by

$$y_{ws3}(t) = a_{31}x_{31}(t,\sigma_{31}) + a_{32}x_{32}(t,\sigma_{32})$$

where $x_{3i}(t,\sigma_{3i})$ is the third order derivatives of Gaussian pulses, expressed by

$$x_{3i}(t,\sigma_{3i}) = \left[\left(\frac{3t}{\sqrt{2\pi}\,\sigma_{3i}^{5}}\right) - \left(\frac{t^3}{\sqrt{2\pi}\,\sigma_{3i}^{7}}\right)\right]\exp\left(\frac{-t^2}{2\sigma_{3i}^{2}}\right)$$

with $i = 1, 2$ and $\sigma_{31} = 55$ ps and $\sigma_{32} = 49$ ps. The Fourier transform of $y_{ws3}(t)$ is given by

$$Y_{ws3}(f) = a_{31}X_{31}(f,\sigma_{31}) + a_{32}X_{32}(f,\sigma_{32})$$, where

$$X_{3i}(f,\sigma_{3i}) = (j2\pi f)^3 \exp\left(-\frac{(2\pi f\sigma_{3i})^2}{2}\right)$$

Based on the above analysis, in Fig. 11, we show the experiment setup to generate and transmit IR-UWB over 100 metres of GI-POF. The generated signal is used to directly modulate a DFB laser at 1302 nm wavelength.

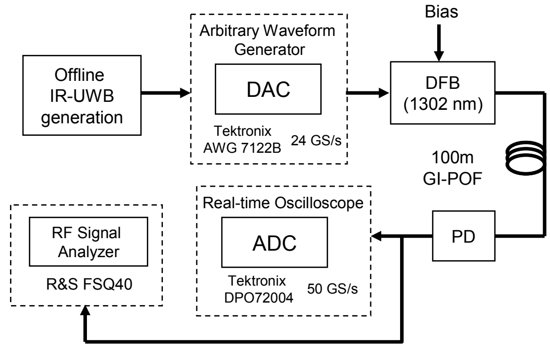

Fig. 11 Transmission experiment setup

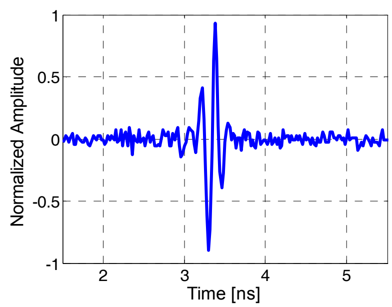

Fig. 12 Generated IR-UWB (electrical back-to-back)

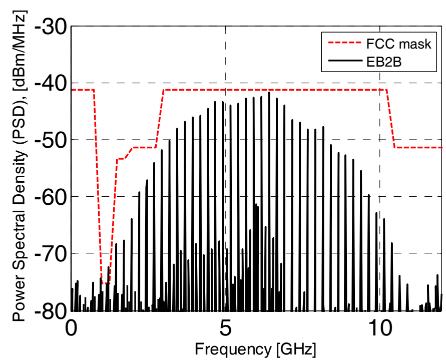

Fig. 13 Spectrum of the generated IR-UWB

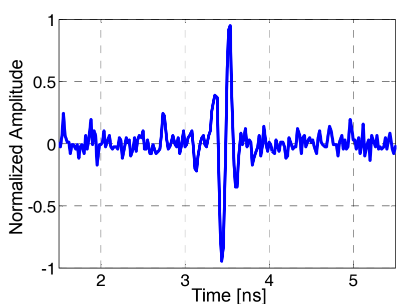

Fig. 14 IR-UWB waveform after transmision

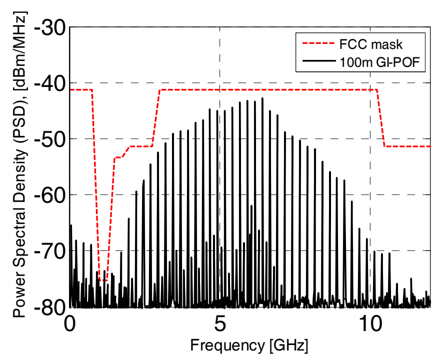

Fig. 15 Spectrum of the received IR-UWB after 100-m GI-POF

The modulated signal is then transmitted over 100 metres of 50-µm core perfluorinated GI-POF and detected by a 25-µm photo-detector (PD). Based on the principle above, IR-UWB pulses have been constructed off-line using MATLAB and copied to the AWG. We use a real-time oscilloscope running at a sampling rate of 50 GSamples/s to show the time-domain waveform and an RF spectrum analyzer to present the IR-UWB spectrum.

The waveform of the generated IR-UWB signal based on the combination of two 3rd order derivatives of Gaussian pulses discussed above is shown in Fig. 12. In Fig. 13, we can see that the spectrum of the generated IR-UWB is fully compatible with FCC mask, which has a central frequency of 6.44 GHz and a 10-dB bandwidth of 5.96 GHz. The spectrum is discrete because of the 250 MHz repetition rate of the AWG. It is also observed that spectral components above 7 GHz are attenuated, which is due to the frequency response of AWG.

After 100-m transmission, the time-domain waveform is shown in Fig. 14. There is no degradation after POF transmission except the attenuation due to the fibre and coupling losses. Fig. 15 finally shows the spectrum of the received IR-UWB signal after transmission. The signal spectrum is still very nicely fitting into FCC mask without much distortion due to the POF transmission. However, a few unstable spectral lines appear below 0.9 GHz after transmission, probably due to random mode mixing effects in the GI-POF. The decrease at the high end of the spectrum in Fig. 15 is due to the limited bandwidth of the GI-POF link.

Conclusion

We experimentally generated an IR-UWB signal which fully complies with the FCC-indoor spectrum mask, even in the most severely power-restricted band from 0.96 GHz to 1.61 GHz based on a weighted sum of 3rd order derivatives of Gaussian pulses. The experimental results show successful transmission of IR-UWB with fractional bandwidth of about 92% over 100m GI-POF. Furthermore, our proposed IR-UWB over GI-POF has a potential application in high speed short range communications networks such as in-building networks.

References

[1] Robert, et al., IEEE Micro. Mag., (2003).

[2] Chen, et al., IEEE Int. Sym. Circ. Syst, 3, (2002).

[3] Ray, et al., IEEE Rad. Wireless Sym., (2006).

[4] Sheng et al, IEEE Int. Conf. Comm,1,(2003).

[5] Koonen, Opt. Comm. ECOC, (2001).

4.9 High capacity data over SMF/MMF

4.9.1 High capacity data over POF [UoA]

UoA investigated experimentally the influence of connectors on the performance of a VCSEL Based Standard Step-Index POF Link. Generally, step-index plastic optical fibers (SI-POFs) are very attractive transmission media for short area optical networks due to their low cost and ease of installation, minimal maintenance needs, etc. Their main drawbacks are their high optical losses especially at the emission wavelength of fast optical sources – namely Vertical Cavity Surface Emitting Lasers (VCSELs) emitting at the spectral window of 650 nm – and their limited bandwidth due to high modal dispersion. However, as their large core offers a series of benefits in such networks that are by definition low cost, they have drawn a lot of attention over the last few years. A point that has not yet been investigated is the influence of the connectors, in terms of the number and their position in the link. All existing studies perform the experimental investigations and testing assuming a single span of POF without any junctions of any type employed. UoA studied the influence of typical SC connectors on the performance of the link. The analysis shows the sensitivity of the link performance to the exact position of the connectors. The degradation is observed experimentally in SI-POF links and it is much stronger than that observed in silica MMF. A first explanation based on the EMD conditions is proposed for the interpretation of the observed experimental measurements. Typical connection schemes are depicted in Fig. 16.

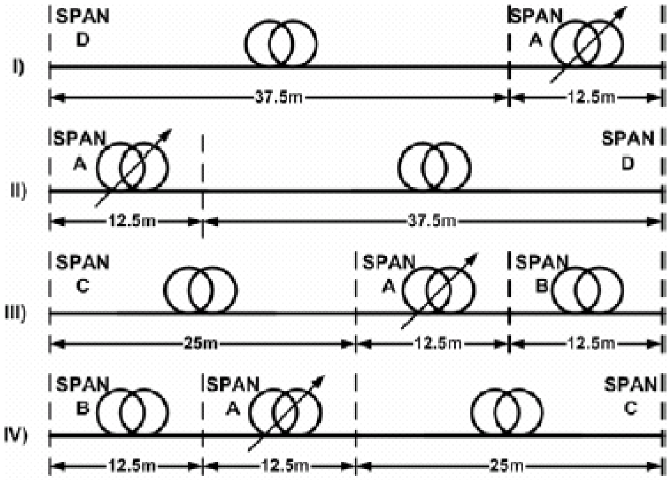

Fig. 16 A 50m SI-POF link consisted of multiple patchcords connected together using SC connectors. A variable number of patchcords of equal length comprise a 12.5m link (Span A) that is placed at different positions of the total link, i) at the end, ii) at the beginning, iii) after 25m, and iv) after 12.5m

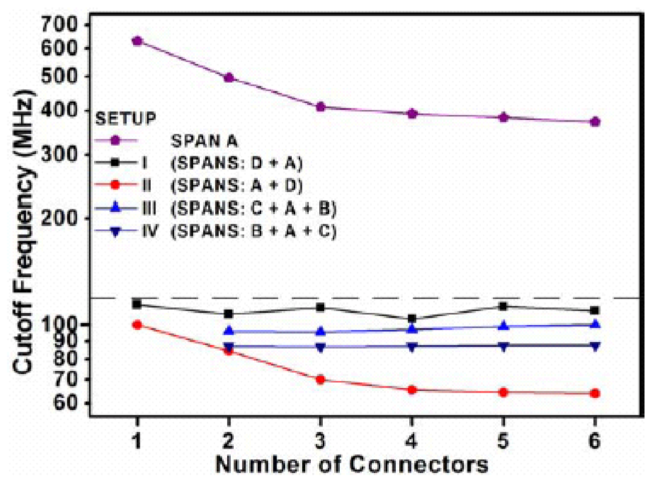

Fig. 17 Cutoff frequency – that corresponds to the -3dB optical bandwidth of a 50m SI-POF link – as a function of the number of connectors used for the various setups shown in Fig. 2. The dashed line indicates the respective frequency of a connector-less 50m link (115MHz). The corresponding bandwidth of a connector-less 12.5m link was found to be over 1GHz.

The frequency response of all setups was acquired with respect to the number of total connectors used in each configuration. A set of measurements was taken for all four setups of Fig. 16. The cut-off frequencies – corresponding to the -3dB optical bandwidth – obtained from the above measurements as a function of the number of connectors employed in each case, are shown in Fig. 17. The multi-connector Span A alone is also shown in the same figure. Regarding Span A, we notice a strong decay of the cutoff frequency with the number of connectors used for the first few connectors introduced. After that point, the cutoff frequency tends to a constant value, i.e. about 400MHz for this instance. The bandwidth of a connector-less 12.5m link was found to be over 1GHz. This behavior indicates that the coupling length is greater than 12.5m, thus the Equilibrium Mode Distribution (EMD) condition is not reached in such a short link when no connectors have been employed. In this case, the introduction of connectors enforces great power redistribution over the modes supported by the POF – about 2 millions – that gets the link closer to the EMD. The excitation of higher order modes results into a stronger modal dispersion and hence a reduced bandwidth.

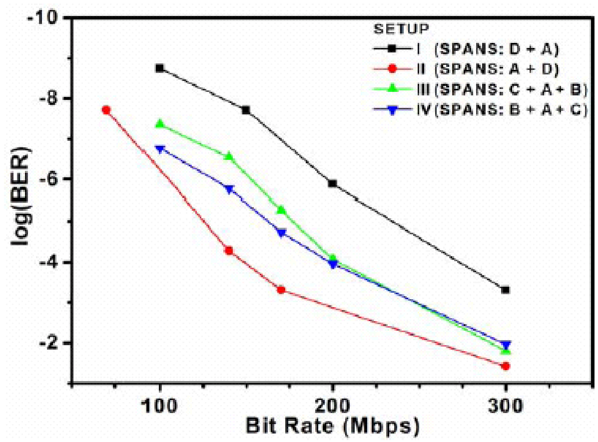

Fig. 18 Bit Error Rate (BER) as a function of bit rate for the various setups. The number of connectors used for this instance is constant and equal to 4

The BER versus the bit rate for a fixed number of connectors and for the various setups considered is shown in Fig. 18. The number of connectors employed is equal to 4 for this instance. The bit rate for a given value of BER increases considerably – almost 2 times for a BER value of 10^{-4} – when the connectors are placed at the receiver end of the link (Setup I), compared to the case where they are placed close to the transmitter (Setup II), as expected.

In conclusion, the influence of the connectors on the performance of the POF based optical link has been experimentally investigated. It was found that the position of the connectors is of major importance resulting in severe degradation of the link performance when these are placed close to the transmitter. This behavior has been attributed to the non satisfaction of the EMD condition in the first part of the transmission link.

UoA is also exploring the performance of Si-POF links carrying multi-level modulation formats (OFDM). The activity aims at defining the bitrate limits of 100 m long POF links and the final results will be obtained till the end of the third year.

Future Activities

UoA's future activities will involve the complete theoretical characterization of a Si-POF based link in terms of their dispersion properties and how those are impaired by the introduction of connectors in different points of the link. We are currently carrying out a theoretical analysis which seems to predict the available experimental findings with a high accuracy. A paper submitted to Journal of Lightwave Technology includes many of the results referring to this activity.

We are also finalizing the evaluation of a complete Si-POF link which incorporates OFDM, electronic equalization and optical methods for the mitigation of the modal dispersion. The activity will be finalized during the last year of the BONE project.

Publications

[1] E. Grivas, D. Syvridis, G. Friedrich, " Influence of Connectors on the Performance of a VCSEL Based Standard Step-Index POF Link," Photonics Technology Letters, vol. 21, No. 4, pp. 1888-1890, Dec. 2009.

4.9.2 Datacommunication links over single-mode fibre and multimode fibre [CAM]

Technologies for low cost data communications are ubiquitous and well established. As the bit rates have increased, much greater demands have been placed on the optical technology involved. For bit rates of 20Gb/s and above, conventional single-wavelength time-division multiplexing (TDM) schemes require high performance components. Wavelength division multiplexing (WDM) circumvents these issues but is typically more expensive since it uses nearly double the component count. Alternatively, advanced orthogonal modulation formats as used in telecommunications have been studied, these involving any of the three orthogonal domains: intensity, phase and polarisation. To date, however, these codes typically require the use of more advanced and expensive optical components, and also may not be suitable for use with multimode optical fibre. In this work, therefore, we propose a dual code modulation scheme using non-return-to-zero (NRZ) and Manchester (MC) codes, which have complementary frequency distributions. NRZ/MC is not only suitable for use with standard datacommunication components and can operate over different fibre types, but also allows lower speed components to be used than in conventional schemes, making it a competitive technique for future low-cost Ethernet systems, for example.

For in-building networks, research has focussed on the emerging standards for enterprise networks, e.g. 40 Gb/s and 100 Gb/s variants of Ethernet. Bandwidth-efficient modulation schemes for MMF and SMF transmission are under development and recent results have been submitting to journals. This novel modulation schemes for SMF and MMF transmission have also been submitted to conferences. Characterisation of high-speed optical devices for such applications has commenced in the last quarter. Analogue characterisation of high-speed optical sources for such applications has commenced recently.

Also detailed activities include:

• Experimental investigation of techniques proposed for radial offset minimisation in MMF connections.

• Experimental demonstration of newly developed optical launch schemes for bandwidth improvement in MMF links. Incorporating two different launch schemes for mode group multiplexed signal transmission over MMF links.

• Dual code modulation scheme, using non-return-to-zero (NRZ) and Manchester (MC) codes, demonstrated both through simulation and experiment.

Publications

[1] S. H. Lee, C. H. Kwok, J. D. Ingham, R. V. Penty and I. H. White."Orthogonal Amplitude-Shift-Keyed Multiplexing for Optical Datacommunication Applications", Proc. IET Meeting on Spectrally Efficient Optical Transmission Systems, London, November 2009.

4.9.3 Real-Time Implementation of a 1.25-Gbit/s DMT Transmitter for Robust and Low-Cost LED-Based Plastic Optical Fiber Applications [TUE, Siemens]

During the last years, the standard step-index polymer optical fibre (SI-POF) with 1-mm core diameter has established itself as the preferred transmission medium for short-range optical data communications in automotive multimedia networks (MOST25/150) with data rates up to 150 Mbit/s. These systems are all based on LED, because of the robustness and stability in terms of temperature behaviour and lifetime in comparison to laser diodes. Due to the rapid integration of numerous multimedia applications in automobiles such as (HD-) DVDplayers, gaming, cameras for monitoring, etc., next generation systems should provide data rates in the Gigabit range while still keeping the LED as optical source. By use of discrete multitone (DMT) [1] or multilevel modulation [2], it has been shown that the severe bandwidth limitations of LED, SI-POF, and large-area photodiode can be successfully overcome for enabling Gigabit transmission. However, until now, only offline signal processing has been used for proving the concept of Gigabit transmission over SI-POF with LEDs.

Below, first results regarding an FPGA-based implementation of a real-time DMT transmitter for 1.25-Gbit/s transmission over SI-POF are presented. A commercial resonant-cavity LED (RC-LED) [3] and a standard PIN photodiode with a large active-area diameter of 540 µm are used for optical transmission and reception respectively.

System Implementation

Fig. 19 shows a functional block diagram of the implementation of the DMT transmitter in FPGA (Xilinx Virtex-4 FX100). A PRBS sequence is generated as input source to the DMT modulator. This serial input sequence is serial-to-parallel converted and mapped onto different quadrature amplitude modulation (QAM) constellation points, implemented using read-only memory (ROM) cells. After this, the parallel QAM symbols are serialized because the pipelined IFFT-core expects serial input data. A demultiplexer (DEMUX) is needed to split the serial data into two parallel processing streams clocked at 312.5 MHz each because the FPGA cannot support a high clock frequency of 625 MHz.

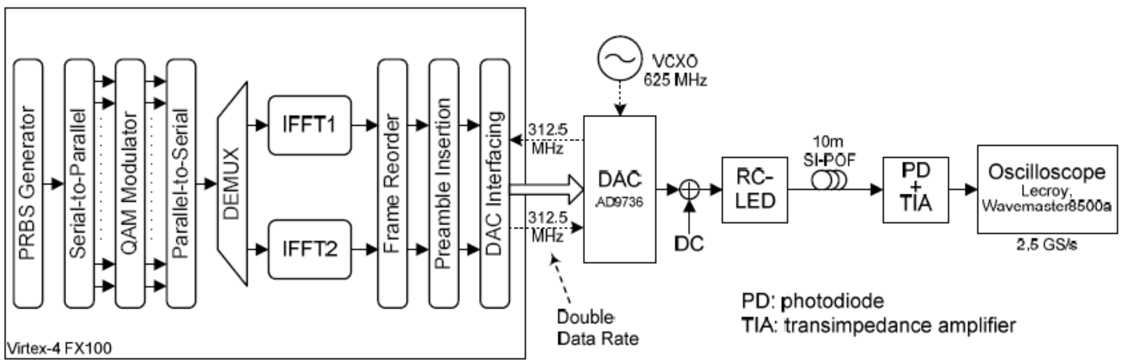

Fig. 19 FPGA implementation of DMT transmitter and experimental setup for performance evaluation

As a result, two IFFT-cores (clocked at 312.5 MHz each) are needed to process the data which is sent to the digital-to-analogue converter (DAC) at double data rate after reordering of the DMT frames and insertion of training preambles. The DAC works at a sampling speed of 625 MSamples/s. Fig. 20 depicts the relative amount of resources needed for each of the functional blocks when everything is implemented using only FPGA slices. A Virtex-4 slice consists of two flip-flops and two 4-input look-up-tables. In the actual implementation, FPGAspecific hardware such as embedded multipliers and block RAMs are used so that full performance can be achieved. As expected, it can be seen from Fig. 20 that the IFFT core demands most resources. Depending on the speed of the DAC and therefore the bandwidth of the DMT signal, parallelization is needed because of limited chip/clocking rate. Higher DAC sampling speeds will require, relatively, more resources for IFFT processing due to the need for parallelization.

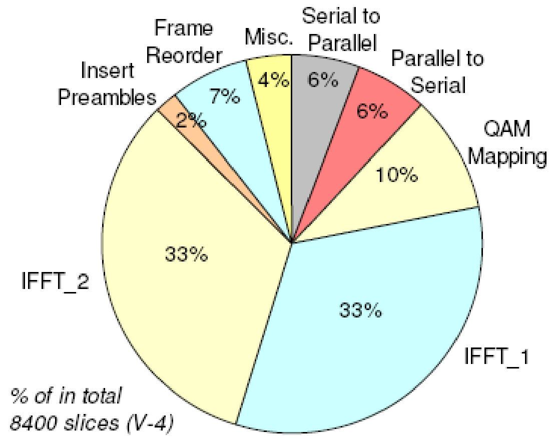

Fig. 20 Virtex-4 FPGA slices utilized in DMT transmitter according to functionality (normalized)

Experimental Results

The experimental setup for evaluating the performance of the DMT modulator is shown in Fig. 19. The DMT sequence generated by the DAC is used to drive an RC-LED for transmission over 10 m of SI-POF. Such distances are typical for automotive networks and the main limitation originates from the low bandwidth of the LED-based transmitter. The received optical power after 10 m SI-POF is -3 dBm and the modulation index is approximately 0.6. A large-diameter (540 μm) photodiode with integrated transimpedance amplifier is used to receive the optical signal and a digital storage oscilloscope sampling at 2.5 GSamples/s is used for demodulation and evaluation of the received DMT sequence. Fig. 21 shows the results of the real-time DMT transmitter. A 128-point IFFT is used for the DMT modulator where the first and last subcarriers are set to 0. Therefore, a total of 62 subcarriers are available and used for information transmission. The bit-allocation is depicted in Fig. 21.a. A 4-point cyclic prefix is used and 10 preambles per 100 DMT frames are transmitted for training and channel estimation purposes. The bandwidth of the DMT signal is approximately 303 MHz, resulting in a bit-rate of 1.25 Gbit/s (1.125 Gbit/s after deduction of preamble overhead). The signal-to-noise ratio (SNR) per subcarrier of the DMT transmitter is measured and plotted in Fig. 21b for both electrical back-to-back and transmission over 10 m SI-POF. The bandwidth limitation of the SI-POF channel can clearly be seen. The spectrum of the DMT signal is measured and depicted in Fig. 21c, where the signal power beyond 312.5 MHz is due to aliasing. This aliasing product is more suppressed in Fig. 21d as a result of the low bandwidth of the SI-POF channel. The received constellation diagrams (after 10 m SI-POF) of the subcarriers as depicted by the arrows in Fig. 3a are plotted in Fig. 21e-h.

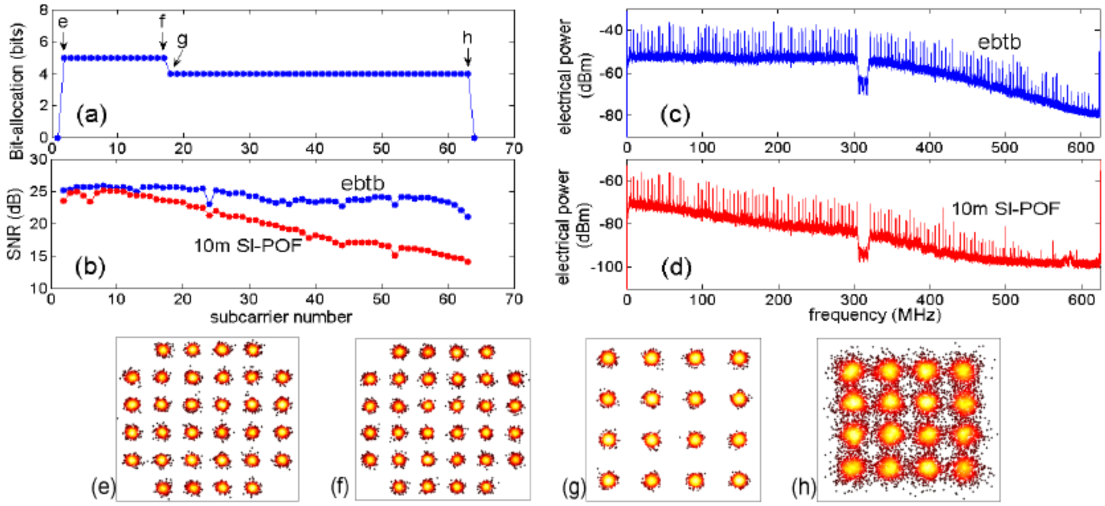

Fig. 21 (a) Bit-allocation per subcarrier. (b) Measured SNR per subcarrier for electrical back-to-back and after transmission over 10 m SI_POF. (c) Spectrum of DMT signal measured at electrical back-to-back and (d) after 10 m SI-POF. (e)-(h) Received constellation diagrams after 10 m SI-POF for subcarriers indicated by arrows shown in (a)

Conclusions

For the first time, a real-time implementation of a 1.25-Gbit/s DMT transmitter has been reported. The performance was evaluated and transmission over 10 m of SI-POF using an RC-LED was successfully demonstrated. This proves that DMT is a promising candidate for upgrading conventional LED-based SI-POF automotive networks to enable Gigabit transmission using standard transceiver and SI-POF.

References

[1] S.C.J. Lee et al., Proc. OFC 2008, paper OWB3

[2] F. Breyer et al., Proc. ECOC 2008, paper We.2.A.3

[3] http://www.firecomms.com/tech-RCLED.html

4.10 Wireless optical communication

4.10.1 High-speed communication using white-light LED lighting systems [FHG-HHI, Siemens]

White LEDs are considered to be a major candidate for future illumination. Due to the potential for simultaneous use of these optical sources for lighting and data transmission, visible-light communications (VLC) have been a subject of increasing research and development activities. Our work was focussed on the experimental investigation of high-speed on-off keying (OOK) transmission using commercially available phosphorescent white-light LEDs.

We demonstrated an indoor visible-light link operating at 125 Mb/s over 5 m distance. In order to compare the performance of OOK against more spectral efficient modulation schemes such as discrete multi-tone (DMT) modulation, we demonstrated the link operating at more than 200 Mb/s by means of digital signal processing which was performed off-line. In both cases, the BERs were sufficiently low to be compensated by forward-error-correction (FEC) mechanisms. The experimental set-up is shown in Fig. 22.

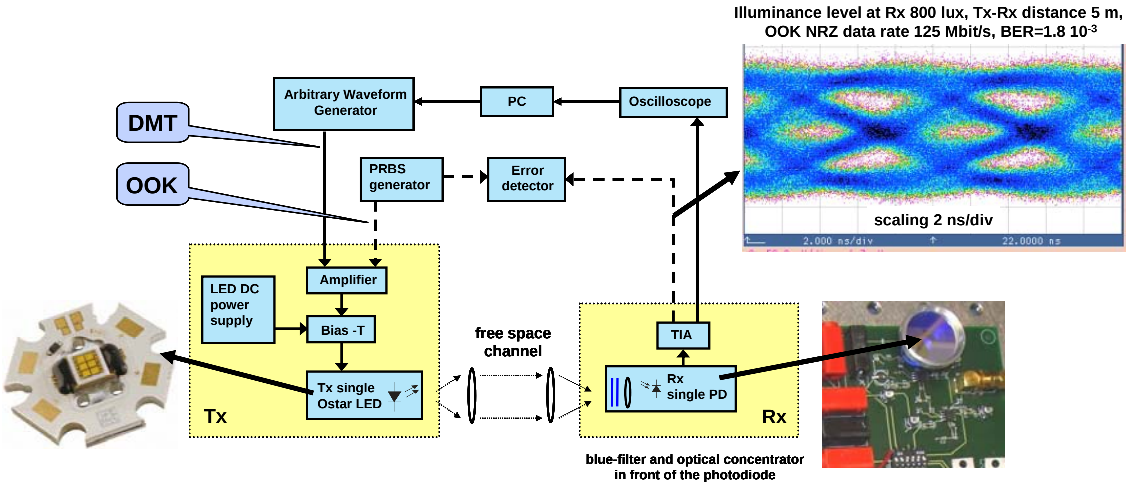

Fig. 22 Setup for transmission experiments over various distances with on-off keying (OOK) and discrete multi-tone (DMT) modulation. The eye diagram was taken from the OOK experiment with 800 lux at the receiver in a distance of 5 m.

The distance between transmitter and receiver units was set to obtain illuminance levels of about 800 and 400 lux, respectively in front of the receiver (sufficient for reading and writing). Such high transmission rates follow from an enhanced modulation bandwidth of the optical system, achieved primarily by blue-filtering in front of the receiver.

Based on the experience from OOK transmission, a signal consisting of 32 subcarriers within a bandwidth of 50 MHz was chosen for the DMT experiments. Since the first input in the IFFT block corresponds to DC, it was left unmodulated. The other subcarriers were modulated with QAM of different orders, i.e. bit-loading was applied, Fig. 23.

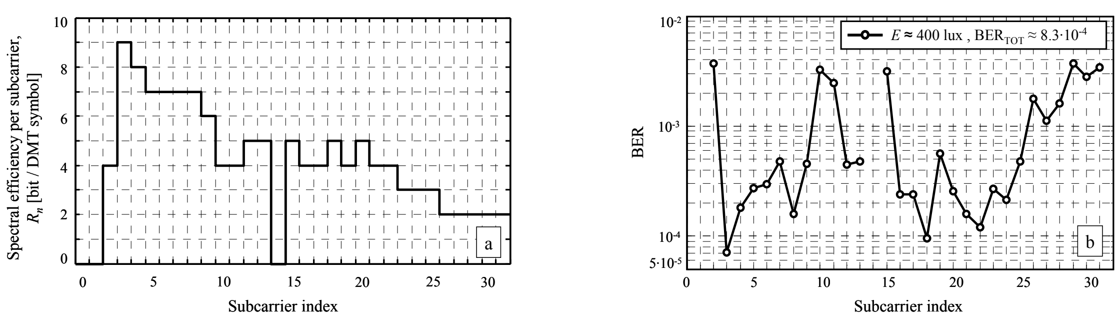

Fig. 23 (a) Bit-loading mask (number of bits per subcarrier in one DMT symbol) for measurements with an illuminance level of ~400 lux at the receiver. (b) Mean BER values over the subcarriers used.

The total gross transmission rate (including redundancy introduced by cyclic prefix and FEC) demonstrated with the bit-loading mask shown in Fig. 23.a was 201.5 Mb/s. The net transmission rate depends on the cyclic prefix length L (in samples) and the FEC coding rate. Given that the visible light channel is rather flat, the cyclic prefix can be kept short. With L = 2 and 7% overhead for the super-FEC assumed, we can expect a resultant net transmission rate of about 182 Mb/s. As the DMT transmission experiments had to cope with adverse conditions of externally induced noise on some subcarriers, we expect significant higher performance in the course of our ongoing work.

4.10.1.1 Future activities

Besides the results reported above and their improvement, there are several areas, which need further research. It is very important to achieve compatibility with illumination technology, where Pulse Width Modulation (PWM) is commonly used for dimming (channel not available during off-periods of the PWM signal). Another important but challenging topic is to provide an efficient uplink to VLC systems. As LEDs often are used in arrays, the application of MIMO techniques also may be of interest. Moreover, new applications appear (such as a combination of VLC technology with energy harvesting, e.g. for sensor applications) and need further work in this area.

4.10.1.2 Joint activities

Collaborative links have been established to a working group at HHI working in the EU projects RIMANA (Radical Innovation MAskless NAnolithography) and MAGIC (MAskless lithoGraphy for IC manufacturing), which have as main focus ultra high-speed (100 Gb/s) optical links. As a result the joint paper [3] has been published, in which an overview of the possibilities for optical free-space communication systems regarding especially industrial applications was given.

Moreover a link has been established to the COST IC0802 group on “Propagation tools and data for integrated Telecommunication, Navigation and Earth Observation systems”. Optical wireless technologies are considered there too, and it is intended to identify items for joint activities.

4.10.1.3 Joint publications

[1] K.-D. Langer, J. Vučić, C. Kottke, L. Fernández del Rosal, S. Nerreter, J. Walewski: Advances and prospects in high-speed information broadcast. Proc. ICTON 2009, Paper Mo.B5.3, 2009 (invited).

[2] J. Grubor and K.-D. Langer, "Efficient signal processing in OFDM-based indoor optical wireless links", Journal of Networks, Vol. 5, No. 2, Feb. 2010.

[3] A. Paraskevopoulos, J. Vučić, S.-H. Voß, K.-D Langer: Optical free-space communication systems in the Mbps to Gbps range, suitable for industrial applications", Proc. IEEE ISOT 2009, pp. 377-382.

4.10.1.4 Presentations

- K.-D. Langer, "Broadband Home Area Networks – Meeting the needs of today and tomorrow", VII Symposium On Enabling Optical Networks and Sensors, Lisbon, June 2009 (invited).
- K. Langer, J. Vučić, C. Kottke, L. Fernández del Rosal, S. Nerreter, J. Walewski, "High-Speed Information Broadcast using Phosphorescent White-Light LEDs – Advances and Prospects", IPHOBAC Workshop 2009, Duisburg, May 2009 (invited).

4.11 Sensor applications

4.11.1 Dynamic Feedback Controlled Harmonic Suppression for Uncooled Dual Function Sensing and Communications Radio over Fibre Link [CAM]

Radio over fibre has been suggested as a possible replacement for co-axial cables for indoor antenna remoting in wireless communications networks. Due to the wide bandwidth available in optical fibre multiple wireless services can be simultaneously carried on a single optical link allowing a single optical fibre to replace several co-axial links. The low attenuation of optical fibre also allows signals to be carried over longer distances than are achievable with co-axial cables. This allows all wireless base stations and access points used within a building to be co-located bringing cost advantages due to the ease of maintenance. Research into radio over fibre links for wireless communications has resulted in the commercialisation of the technology with a wideband 370 MHz – 2.7GHz system recently becoming available. Besides the reduction in maintenance costs radio over fibre distributed antenna systems have been demonstrated to reduce the overall power output to provide a given area of coverage compared to a single antenna system. The reduction in output power reduces inter-cell interference, increases the data capacity and could enhance battery life in the mobile terminal.

However, interest has also been increasing in wireless sensor networks. The use of RFID tags will in the future allow ‘an internet of things’ allowing objects to be automatically identified, associated with information and other objects. For many applications, passive UHF RFID operating in the 900MHz is emerging as the technology of choice due to the low cost, battery-less tags. The tag is powered by a high power RF carrier in the far field of the reader, and tag to reader communication is achieved by backscatter modulation of the carrier. Typical current systems have a read range of around 10m.

To date, RFID systems have been developed consisting of readers distributed at the desired read points, using a digital communications backhaul to some middleware platform where information in inferred from the tags read. However, with the constant contraction in cell size in communications networks to support more users at higher data rates it is conceivable that soon, the antenna spacing requirements for RFID and communications will be the same. Therefore it is desirable to be able to support both passive UHF RFID and communications on the same optical distribution network allowing RFID to leverage the coverage advantages which have been brought to communications services through optical DAS, and at the same time benefit from hardware co-location and reductions in maintenance costs.

To reduce the power consumption of the tag, the bandwidth is typically low typically around 100kHz, and the transmitted power very high around +30dBm to ensure sufficient power to power the tag after free space losses. This is 10-20dB greater than the transmitted power used for wireless communications. The high power carrier required in the downlink has the potential to induce non-linear distortion in the laser diode when direct modulation is used. Due to the narrow bandwidth, the third order inter-modulation is not a problem, however, in a broad band system supporting all the major communications frequency bands, the second harmonic will fall in-band, and will be transmitted. To reduce the effects of such spurious emissions on other wireless services, regulations limit the permitted output power of these spurious emissions.

As the second harmonic will increase at twice the rate of the fundamental with increasing input RF power, if only the RFID service is to be supported on the RoF link, the input power can be reduced to maintain the second harmonic at acceptable levels. However, if communications services are to be supported alongside the RFID signals, the required difference in output power and SNR of the communications service can impose restrictions on the lowest modulation power which meets the requirements of the communications service.

In a conventional system, the second harmonic may be filtered before the transmission antenna, however in a multi-service optical DAS it is desirable to maintain the system transparency and not make changes at the antenna units. Instead a cancellation scheme may be employed at the optical transmission end of the radio over fibre link. Since the RFID band is narrow, there is no need to provide harmonic suppression across the entire system bandwidth. Therefore we concentrate on a narrow band system.

If the laser generated second harmonic is considered to have an amplitude equal to A and a phase of ϕ, then the idea cancelling signal will have an amplitude equal to A and a phase of $\phi + \frac{\pi}{2}$ resulting in complete cancellation. However if the amplitude is instead $A + \delta A$ and the phase $\phi + \delta\phi$ then the magnitude of the resulting harmonic will be:

$$E^2 = 2A^2 + 2A\delta A + \delta A^2 - 2(A^2 + A\delta A^2)\cos\delta\phi$$

The equation is plotted in Fig. 24 giving the harmonic suppression as a function of amplitude and phase error in decibels. A high degree of accuracy is required to achieve a high level of suppression.

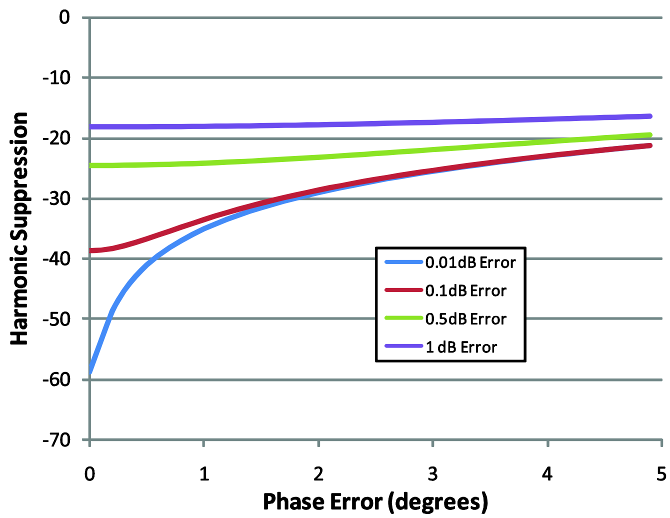

Fig. 24 Level of harmonic suppression with errors in the amplitude and phase of the compensating signal

A low cost electronic harmonic cancellation scheme was previously proposed. An electronic frequency doubler, variable attenuator and phase shifter generate the out of phase cancelling signal. It was shown that the use of electronic feedback of the amplitude and phase of the resultant harmonic signal can overcome the non-linearity of low cost electronically variable attenuators and phase shifters and the lack of independence of the adjustment of phase and attenuation. The system is shown in Fig. 25.

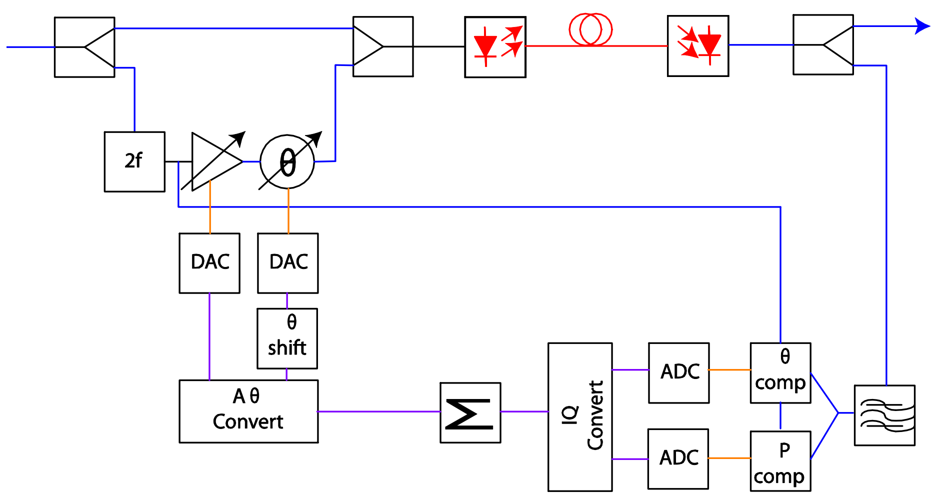

Fig. 25 A low cost electronic harmonic compensation scheme with feedback

It was also noted that there were fluctuations in the level of the second harmonic. Due to the high requirement for accuracy of the amplitude of the compensating signal, fluctuations in the harmonic output are problematic to the cancellation scheme. Here we demonstrate that feedback control of the harmonic output can be used to enhance the performance of an uncooled laser with a fluctuating harmonic output.

Harmonic distortion arises due to a number of reasons namely 2nd order interactions of the rate equations , optical reflections and spatial hole burning . As a result in an uncooled laser, the harmonic output is more variable than the output power of the fundamental. The harmonic output is also expected to vary with laser ageing. Fig. 26 shows a plot of the second harmonic power of an uncooled DFB laser followed by an optical isolator to reduce reflections measured at 1.736GHz under 868MHz modulation. It can be seen that over the 100 second measurement period, the harmonic varies by 1.6dB peak to peak. From equation 1 it can be inferred that the maximum achievable harmonic suppression is 13dB assuming that there are no phase variations accompanying the amplitude variations.

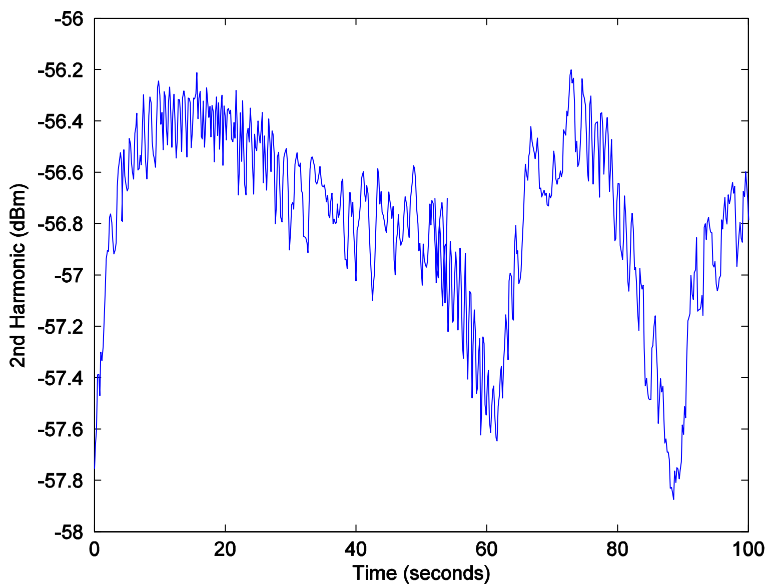

Fig. 26 Power variation of the 2nd Harmonic of an uncooled directly modulated DFB laser

The feedback controlled suppression system used in has the potential to partially overcome the variation in the laser harmonic output variation by allowing the cancelling signal to track the changes. As the feedback look has a sampling interval of 1.7kHz limited by the low cost microcontroller used to implement the control algorithm, only fluctuations which are significantly slower than the update rate can be corrected. It can be seen from Figure 3 that while there are fast variations, the largest swings occur over a number of seconds.

To determine the performance advantage offered by dynamic control of the compensating signal as opposed to static control, the control system was first allowed to settle from its start up dynamics, and the state of the amplitude and phase control frozen for 100 seconds while the second harmonic is recorded. The experiment is then repeated with the controller allowed to vary the amplitude and phase output. Fig. 27 shows the level of the second harmonic under the two regimes. It can be seen that the use of full feedback control results in an additional 6dB suppression of the second harmonic.

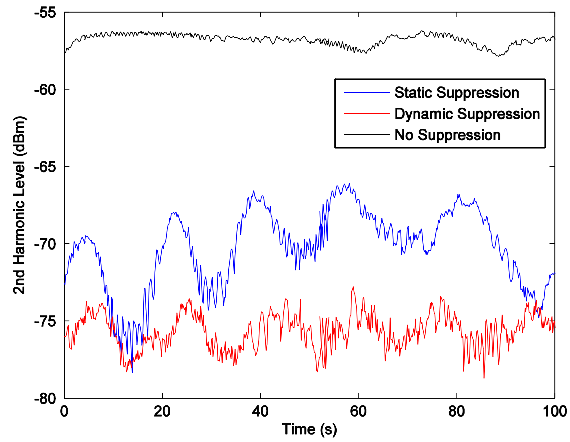

Fig. 27 Comparison of the second harmonic with static and dynamic control of the control of the compensating signal

Thus, in radio over fibre systems using uncooled lasers, the level of harmonic suppression achievable by feed-forward of an electronically generated second harmonic can be limited by instability of the laser generated second harmonic distortion. The use of feedback of the amplitude and phase of the resultant second harmonic can overcome this problem and result in 6dB greater suppression.

Publications

[1] F. Yang, M. Crisp, K. Fang, R. V. Penty and I. H. White, "Silicon Avalanche Photodiodes for Low Cost, High Loss Short Wavelength Radio Over Fiber Links", in Proc. CLEO 2009.

[2] S. Sabesan, M. Crisp, R. V. Penty and I. H. White, "Demonstration of Improved Passive UHF RFID Coverage using Optically-Fed Distributed Multi-Antenna System", in Proc. RFID 2009.

[3] M. Crisp, S. Sabesan, R. V. Penty and I. H. White, "Dynamic Feedback Controlled Harmonic Suppression for Uncooled Dual Function Sensing and Communications Radio over Fibre Link", in Proc. ICT-Mobile Summit 2009.

[4] F. Yang, M. J. Crisp, K. Fang, R. V. Penty, and I. H. White, "Short Reach Radio over Polymer Fibre Links", in Proc. ECOC 2009.

[5] K. Fang, M. J. Crisp, F. Yang, R. V. Penty and I. H. White "Demonstration of Distributed Antenna System Using Optical Multicast Radio-over-Fibre Links" in Proc. MWP 2009.

[6] T. Li, M. J. Crisp, R.V. Penty and I. H. White, "Low Bit Rate Digital Radio over Fibre System", in Proc. MWP 2009.

[7] M. Crisp, S. Sabesan, R.V. Penty and I.H. White, "Mixed Wireless Communications and RFID Sensor Networks over Fibre", in Proc. AVFOP 2009 (invited).

4.11.2 Sensor applications in-home networks [UC3M, UDE, Ericsson]

Recently, Polymer Optical Fibers (POF) has been widely used in industry and automotive networks. New technologies and applications like VDSL, FTTH and IPTV require reliable high-speed but low cost networks with simple installation, high security and low space consumption [1] . POF technology can satisfy these requirements [2] and, hence, hence, in-home POF based networks are currently being installed.

In the optical sensing field, POFs are also experiencing a big growth because they present numerous advantages such as easier handling (more flexibility) and lower cost compared to glass optical fibers. These are some reasons why new POF sensors have appeared and are still appearing, most of them based on optical power intensity detection.

In the framework of this network, a novel self-referencing fiber optic intensity sensor based on bending losses of a partially polished polymer optical fiber (POF) coupler has been characterized for determining its robustness to temperature fluctuations in a climatic chamber. The coupling ratio (K) depends on the external liquid in which the sensor is immersed. It is possible to distinguish between different liquids and to detect their presence. Experimental results for the most usual liquids found in industry, like water and oil, are given. K value increases up to 10% from the nominal value depending on the liquid. Sensor temperature dependence is studied for a range from 25 ºC (environmental condition) to 50 ºC. Any sector requiring liquid level measurements in flammable atmospheres can benefit from this intrinsically safe technology [3] .

References

[1] T. Koonen, “Fiber to the Home/Fiber to the Premises: What, Where and When?” in *Proc. of the IEEE*, Vol. 94, Issue 5, May 2006 pp. 911–934.

[2] Sebastian Randel et al., “1 Gbit/s Transmission with 6.3 bit/s/Hz Spectral Efficiency in a 100 m Standard 1 mm Step-Index Plastic Optical Fibre Link Using Adaptive Multiple Sub-Carrier Modulation”, *32nd European Conference and Exhibition on Optical Communication ECOC 2006*, paper Th4.4.1, 24.-28.09.2006, Cannes, France.

[3] D.S. Montero, C. Vázquez, I. Möllers, J. Arrúe, D. Jäger "A Self-referencing Intensity Based Polymer Optical Fiber for Liquid Detection Sensors" *Sensors* (Special Issue State-of-the-Art Sensors Technology in Spain), 9 (8), 6446-6455, 2009

Outcome of the joint research activity:

- Joint paper (ref. [3])

4.12 Techno-economic analysis

4.12.1 Optimisation of In-Building Optical Networks [TUE, FT]

With FTTH techniques being rolled out at increasing pace in access networks, offering unprecedented bandwidths to residential homes, the next challenge is to get these bandwidths into the homes themselves[1] [2] . Inside residential homes and (semi-)professional buildings, currently a wide variety of networks is deployed: twisted copper pairs for telephony and fax, coaxial cables for CATV and radio broadcast signals, Cat-5 cables for connecting computers and other IP-based terminals, wireless LAN for laptop computers, PDA-s and gaming consoles, dedicated cables for domotica applications, etc. The maintenance and upgrading issues associated with this jungle of networks could be considerably simplified by replacing all of them by a single integrated multi-services network.

Optical fibre with its huge bandwidth and transparency for all kinds of signal formats is uniquely suited as the transport medium in such an integrated network. Silica single-mode fibre (SMF) offers the ultimate performance, but requires precision tools and skilled personnel for installation. Silica multi-mode fibre (MMF) with its larger core is easier to install; silica graded-index multimode fibre has a high bandwidth and has already been installed widely in office buildings. Large-core polymer optical fibre (POF) with its large ductility is even easier to install; ∅1mm-core PMMA step-index POF is well suited for do-it-yourself installation by residential home owners. Gigabit Ethernet transport using a low-cost LED over 50 metres of 1mm PMMA SI-POF has been demonstrated [3] . Also high-capacity wireless microwave signals can be delivered over multimode fibre by the dispersion-robust optical frequency multiplying technique [4] .

Network architectures

The optical fibre integrated network can basically be laid out in a number of architectures, as shown in Fig. 28. The connection from the access network to the in-building network is made via the Home Communication Controller (HCC), which acts as a gateway and can perform many signal translation and network control functions. In the point-to-point (P2P) architecture, individual fibres run from the HCC to wall outlets in each room. The tree and bus architecture are point-to-multipoint (P2MP) architectures, which can be optically transparent when the splitting nodes do optical power splitting or wavelength routing, or opaque when the nodes internally do O/E/O conversion. The star architecture is multipoint-to-multipoint (MP2MP), and allows direct communication between the wall outlets in different rooms without the intervention of the HCC; this can be done all-optically if the star coupler is a reflective optical coupler.

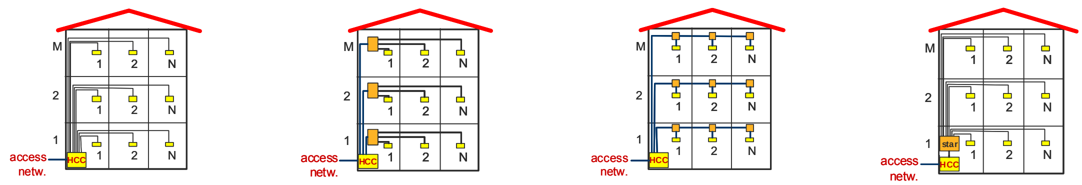

a) point-to-point (P2P) b) tree c) bus d) star

Fig. 28 Network architectures

An assessment has been made of the costs of installing these architectures. When the star coupler is installed next to the HCC, the costs of the star network are similar to those of the P2P network. Fig. 29 shows a comparison of the installation costs of the P2P, the tree and the bus architecture, for a low-rise building (M=3 floors) and a high-rise one (M=10 floors) versus the number of rooms N per floor. The parameters assumed were: room height H=3 metres, room length L=5 metres, fibre cable costs of 3€/metre, costs of installed duct for a single fibre cable 15€/metre (and increasing with the square root of the number of cables in it). The network nodes were assumed to cost €20 for a 1x2 splitter, and €15 per port for a 1xN splitter ($N \geq 3$).

As illustrated by Fig. 29, for small buildings (low-rise, with M=3 floors and $N \leq 3$ rooms/floor), the cost differences between the architectures are relatively small. For larger buildings, in particular for high-rise (M=10) buildings with a large number N of rooms per floor, the bus architecture is clearly more cost-effective than the P2P and tree ones.

Regarding the fibre type, multimode (silica or polymer) fibre is much less suited than single-mode fibre for P2MP and MP2MP architectures, as power splitters and wavelength routers are hard to realize with multimode fibre (bulk-optics solutions may be devised, carefully trying to avoid mode-selective processes which generate modal noise).

Regarding service upgrading, and regarding the simultaneous support of high-capacity wired services as well as wireless services (by radio-over-fibre techniques), all-optical networks are preferred above opaque ones as they provide end-to-end signal format transparency and thus easily allow modifications in the transported signals.

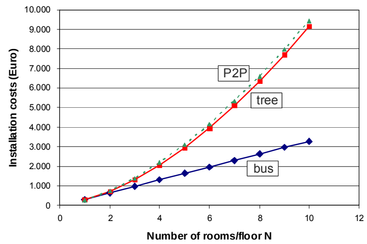

a) M=3 floors

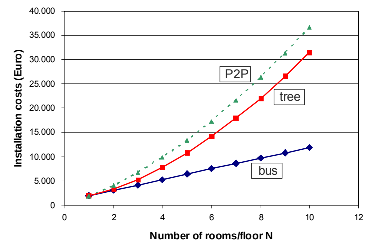

b) M=10 floors

Fig. 29 Comparison of installation costs

Architecture selection

From the above, one may conclude that for smaller buildings (e.g. residential homes) a P2P architecture using do-it-yourself POF techno-economically is the best choice. It obviously provides signal transparency from the HCC to every wall outlet. Scaling to more wall outlets can be achieved all-optically by installing extra POF-s, or opaquely by adding O/E/O network splitting nodes interconnected with POF.

For larger buildings, P2MP architectures are techno-economically more attractive, in particular a bus architecture. An all-optical P2MP architecture using SMF offers the best prospects for upgrading and for support for both wired and wireless services.

All-optical bus topology with weighted couplers

When using identical optical tap couplers, a bus architecture requires a large dynamic range of the receivers in the user terminals as the optical power available at the first terminal differs considerably from that at the last terminal. Reversely, when the transmitters in the terminals emit at the same power level, the burst mode receiver at the HCC needs to have a wide dynamic range. These power level differences between the terminals can be significantly reduced when all tap couplers do not have the same tap ratio. As shown in Fig. 30, the power tap ratio p_i of the i^{th} coupler should be adjusted such that the tapped power P_0 is equal at all nodes.

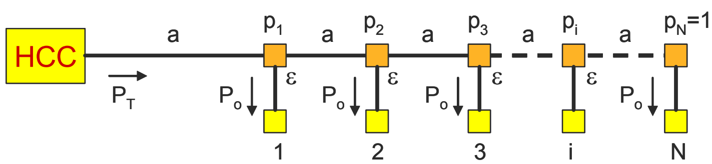

Fig. 30 Weighted tap couplers in a bus

When assuming that the fibre links between the couplers all have a power loss fraction a, and each tap coupler has an excess loss ε, this tap ratio p_i is

$$p_i = 1 - \left(1 + a^{N-i} \varepsilon^{N-1-i} \prod_{j=i+1}^{N-1} (1 - p_j)\right)^{-1}$$

with i = 1 .. (N-2) and p_N=1, p_{N-1}=1-1/(1+a). E.g., for a bus with N=10 taps, the optimized tap ratio per coupler is shown in Fig. 31. For nearly lossless fibre links ($a \cong 1$) and lossless couplers ($\varepsilon \cong 1$), we find $p_i \cong 1/(N-i+1)$ and $p_1 \cong 1/N$, so $P_0 \cong P_T / N$. Hence in the lossless approximation the weighted-taps bus performs as efficient as a lossless 1:N power splitter. Thus, when using weighted tap couplers, the bus architecture does not put higher requirements on the dynamic range of the terminal equipment than the star and tree architectures do, and simultaneously saves on costs for fibre cabling and duct space.

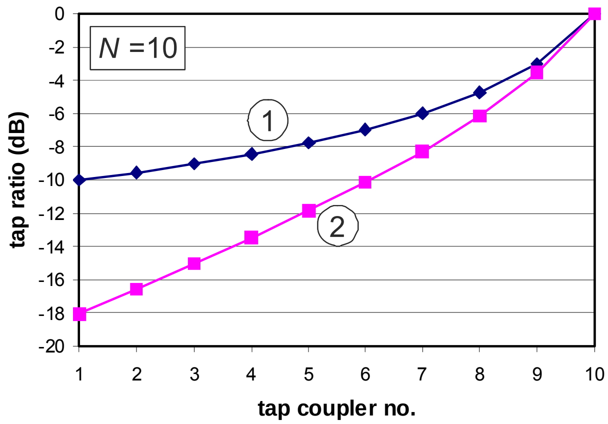

Fig. 31 Optimum tap ratio per coupler (① for loss-free couplers and fibre links; ② for a = -1dB and ε = -0.5dB)

Conclusions

Taking the economics and the potential for upgrading and for integrated delivery of services into account, POF-based P2P architectures are optimum for smaller (residential) buildings, whereas SMF-based bus architectures are the best choice for larger (professional) buildings. By using weighted tap couplers in the bus line, the required dynamic range of the terminals can considerably be reduced.

References

[1] P. Chanclou et al., Proc. ECOC'08, We3F1 (2008)

[2] A.M.J. Koonen, Proc. ECOC'08, We2A1 (2008)

[3] S.C.J. Lee et al., Proc. OFC'08, OWB3 (2008)

[4] A.M.J. Koonen, M. García Larrodé, J. Lightwave Technol. **26**, 2396-2408 (2008)

4.13 Safety and health aspects

No activities of partners reported.

5. Mobility actions

UC3M – GET:

- PhD student Pedro Contreras from UC3M has spent more than 3 months in Telecom Bretagne: 18 Sep.-28 Nov. 2009
- Prof. C. Vázquez & B. Fracasso discussions at 2 days visit at Telecom Bretagne of C. Vázquez (February 2009) and 3 days visit at UC3M of B. Fracasso. K.Hegartty (April 2009)
- A mobility action from R. Chandy to UC3M for further discussions for selecting another sensor to be developed and tested
- A new mobility from Prof. C. Vázquez to Telecom Bretagne will be done on February 2010

UAM – TUE:

- Post-doctoral researcher dr.ir. Bas Huiszoon, for 2 weeks to do incoherent spectral OCDMA system measurements at TUE

Ericsson – UDE:

- PhD student to work on POF devices at UDE

6. Joint publications

In 2009, by WP16 partners 8 joint publications have been made, and 26 single-institution papers. The full list is given at the BONE website, https://ict-bone.unibo.it/all_papers.php?per=8&wp=WP16 .

7. Joint workshops

In order to establish the dissemination of knowledge built up in the joint activities, and to discuss new joint activities, a joint WP13/WP16 workshop has been held at the BONE general meeting in Poznan, Oct. 5. ve been held in this first year:

WP16 researchers have contributed to many other workshops and conferences by disseminating the jointly built knowledge, amongst others at OFC 2009 in San Diego, NOC 2009 in Valladolid, ECOC 2009 in Vienna, MWP 2009 in Valencia.

8. Concluding remarks and future plans

In BONE's second year, in WP16 the cooperation between the partners has been intensified, notably by cooperation through mobility actions. As a result, amongst others, joint proposals have been prepared for the Call 5 of FP7.

In 2010, the final year of BONE, WP16 activities are planned to focus on extending the cooperation through mobility actions further, and also on producing more joint publications resulting from these. The partners have jointly made proposals for new research projects, amongst others in response to FP7 Call 5. As a result, it is expected that the cooperation between WP16 partners will continue after the final year of BONE. Thus WP16's activities will lead to a lasting framework for Europe-wide interaction in research in the domain of in-building networks, thus enhancing the worldwide visibility of Europe's research and contributing to strengthening the position of Europe's industrial and academic activities.

Annex 1: Partner interests in VCE-H key research topics

		P4	P6	P12	P16	P17	P18	P22	P23	P36	P45	P49
		FHG-HHI	UDE	UC3M	UVIGO	FT	GET	UoA	UoP	TUE	UCAM	Ericsson
1	**In-building optical network architectures,** for integration of services, wired and wireless	X	X		X	X	X	X	X	X		
2	**Hybrid (optical/copper/wireless) in-building networks,** upgrading strategies, network evolution	X	X	X	X	X	X	X		X	X	
3	**Management and control of in-building networks,** ambient intelligence, signal routing, control of resources, user-tailored services		X		X					X		
4	**Fault & performance monitoring + protection mechanisms,** assure QoS, ease of maintenance, service availability	X										X
5	**Gateways access/in-building;** interfacing, security, service adaptation, local server, …	X	X						X			
6	**Interfacing with user terminals,** matching I/O formats		X									
7	**Flexible capacity allocation,** capacity and QoS on demand								X	X		

8	**Radio-over-single/multimode fibre,** antenna remoting, central station consolidation, smart antennas		X	X		X	X	X		X	X	
9	**High capacity data over SMF/MMF,** BW efficient modulation formats, such as multilevel, QAM, …; dispersion compensation	X	X	X		X		X	X	X	X	
10	**Optical wireless communication,** for pico-cells	X	X		X		X			X		
11	**Sensor applications** (bursty, low data rate, multiple access)		X	X	X							X
12	**Techno-economic analysis,** to optimise system design and network architecture		X			X						X
13	**Safety and health aspects** (a.o. eye safety, automatic shut-down)	X	X	X								X